

Supporting Information

Multiresponsive Dynamic Covalent Assemblies for the Selective Sensing of Both Cu^{2+} and CN^- in Water

Daijun Zha and Lei You*

State Key Laboratory of Structural Chemistry, Fujian Institute of Research on the
Structure of Matter, Chinese Academy of Sciences, Fuzhou 350002, P. R. China

E-mail: lyou@fjirsm.ac.cn

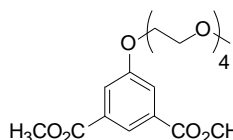
Materials. Anhydrous methanol, anhydrous ethanol, dichloromethane, hydrazine hydrate, N,N-dimethylformamide, and dimethyl sulfoxide were purchased from Sinopharm Chemical Reagent Co., Ltd. CDCl_3 and $\text{DMSO-}d_6$ were purchased from Aldrich. All other reagents were obtained from commercial sources and were used without further purification, unless indicated otherwise.

Instruments and Measurement. $^1\text{H-NMR}$ spectra were recorded on a 400 MHz Bruker Biospin avance III spectrometer. The chemical shifts (δ) for ^1H NMR spectra, given in ppm, are referenced to the residual proton signal of the deuterated solvent.

Gel permeation chromatography was run on a Waters 1515 high performance liquid chromatography instrument equipped with a 2414 differential refractometer and a set of Styragel mixed-C columns (Styragel Waters HR4E and HR5E) to separate molecular weights ranging from 10^2 to 10^6 . The oven temperature was set at 40°C . THF was used as the eluent, and the flow rate was 1 mL/min. Monodispersed polystyrene standards (Aldrich Chemical Co.) were used to generate the calibration curve.

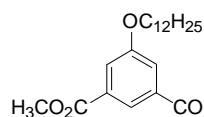
UV/Vis spectra were recorded on a Lambda 35 spectrophotometer. Deionized water was used for the titration. Upon addition of acid, base, or analytes, each sample was allowed to equilibrate before the spectrum was recorded. The corresponding binding isotherm was generated.

concentrated *in vacuo* to a small volume, and the residue was dissolved in EtOAc. The organic layer was washed with 5% aqueous NaHCO₃ and brine. The combined aqueous layers were extracted with EtOAc. The combined organic layers were dried over Na₂SO₄, and evaporated. The crude product was crystallized from EtOH in 80% yield as a white crystalline solid. ¹H NMR (400 MHz, CDCl₃): δ = 8.29 (s, 1H), 7.76 (s, 2H), 5.62 (s, 1H), 3.97 (s, 6H).

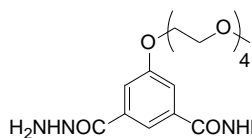


The methyl tetraglycol tosylate (0.36 g, 1 mmol) and 3, 5-di(methoxycarbonyl)phenol (0.24 g, 1.05 mmol) were dissolved in anhydrous DMF (40 mL). K₂CO₃ (1.38 g, 10 mmol, 10.0 equiv) was added, and the reaction mixture was heated at 90 °C for 24 h. After cooling to room temperature, the reaction mixture was extracted with H₂O and CH₂Cl₂. The aqueous phase was washed three times with CH₂Cl₂. The combined organic phases were washed three times with water, dried (Na₂SO₄), and evaporated. The crude product was purified by column chromatography (EtOAc/hexane, 30: 70) to afford the compound as colorless oil in 85% yield. ¹H NMR (400 MHz, CDCl₃) δ = 8.30 (s, 1H), 7.79 (d, J = 1.2 Hz, 2H), 4.33-4.18 (m, 2H), 3.96 (s, 6H), 3.93-3.88 (m, 2H), 3.76 (dd, J = 6.2, 3.5 Hz 2H), 3.68 (ddd, J = 9.4, 5.6, 3.1 Hz, 8H), 3.56 (dd, J = 5.6, 3.7 Hz, 2H), 3.39 (s, 3H). ¹³C NMR (400 MHz, DMSO-d₆): 165.62, 159.27, 131.94, 122.25, 119.81, 71.74, 70.46, 70.30,

70.28, 70.24, 70.04, 69.23, 68.47, 58.46, 52.94.

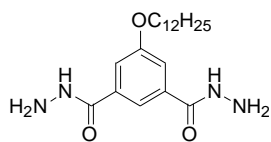


A stirred mixture of 3,5-di(methoxycarbonyl)phenol (2.24 g, 10 mmol) in 100 mL anhydrous DMF with K_2CO_3 (5.52 g, 40 mmol) was heated at 90 °C for 30 min, and 1-bromododecane (2.8 g, 11 mmol) in 10 mL DMF was then added over 15 min. The reaction was monitored by TLC until the starting materials completely disappeared. After cooling to room temperature, the reaction mixture was extracted with H_2O and CH_2Cl_2 . The aqueous phase was washed three times with CH_2Cl_2 . The combined organic phases were washed three times with water, dried (Na_2SO_4), and evaporated. The crude product was purified by column chromatography (EtOAc/hexane, 20: 80) to afford the compound as a white powder in 80% yield. 1H NMR (400 MHz, $CDCl_3$) δ = 8.28 (t, J = 1.4 Hz, 1H), 7.76 (d, J = 1.4 Hz, 2H), 4.06 (t, J = 6.5 Hz, 2H), 3.95 (d, J = 4.5 Hz, 6H), 1.92-1.76 (m, 2H), 1.53-1.44 (m, 2H), 1.39-1.25 (m, 16H), 0.90 (t, J = 6.8 Hz, 3H). ^{13}C NMR (400 MHz, $CDCl_3$): 166.25, 159.24, 131.67, 122.74, 119.83, 68.62, 52.40, 31.93, 29.67, 29.65, 29.60, 29.36, 29.10, 25.98, 22.70, 14.14.

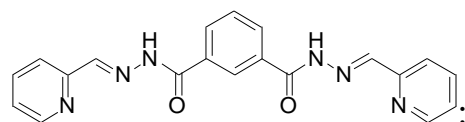


Dimethyl terephthalate methyl tetraglycol (0.4 g, 1 mmol) was dissolved in 15 mL EtOH, and hydrazine monohydrate (1 mL) was added. The reaction mixture was refluxed overnight. The reaction mixture was concentrated *in vacuo* to a small volume after cooling down

to room temperature. The precipitate was filtered, washed with water thoroughly, and dried completely to give 0.22 g white powder (yield 55%). ^1H NMR (400 MHz, DMSO- d_6): δ = 9.79 (s, 2H), 7.87 (s, 2H), 7.49 (s, 2H), 4.51 (br, 4H), 4.19 (t, J = 8 Hz, 2H), 3.78 (t, J = 6 Hz, 2H), 3.61-3.41 (m, 12H), 3.23 (s, 3H). ^{13}C NMR (400 MHz, DMSO- d_6): 165.59, 158.74, 135.22, 118.98, 115.94, 115.66, 71.72, 70.41, 70.27, 70.22, 70.02, 69.24, 68.07, 58.56.

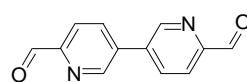


: Use the procedure described above. ^1H NMR (400 MHz, DMSO- d_6): δ = 9.78 (s, 2H), 7.85 (s, 2H), 7.46 (s, 2H), 4.50 (br, 4H), 4.04 (t, J = 6 Hz, 2H), 1.73 (m, 2H), 1.25-1.42 (m, 18H), 0.86 (t, J = 6 Hz, 3H). ^{13}C NMR (400 MHz, DMSO- d_6): 165.59, 158.92, 135.22, 118.72, 115.77, 115.49, 68.36, 29.50, 29.02, 25.94, 22.58, 14.57.



: 1,3-Benzene-dicarbohydrazide (0.194 g, 1 mmol) was added to a MeOH solution (70 mL) containing pyridine-2-carbaldehyde (0.23 g, 2.2 mmol). After 5 drops of acetic acid was added, the yellow mixture was heated at boiling temperature under magnetic stirring for 24 h. During the reaction, yellow precipitate was formed, which was collected by filtration and washed with MeOH thoroughly (0.26g, 70%). ^1H NMR (400 MHz, DMSO- d_6): δ = 12.23 (s, 2H), 8.64 (d, J = 4 Hz, 2H), 8.51 (m, 3H), 8.17 (d, J = 4 Hz, 2H), 8.02 (d, J = 8 Hz, 2H), 7.91 (t, 2H), 7.74 (t, 1H), 7.45 (t, 3H). ^{13}C NMR (400

MHz, DMSO-d₆): 163.24, 153.64, 150.05, 148.96, 137.41, 134.04, 131.57, 129.45, 127.55, 125.00, 120.50. ESI-MS: *m/z* calcd for C₂₀H₁₇N₆O₂ (M + H⁺): 373.1; found: 373.0. Elemental analysis: calcd (%) for C₂₀H₁₆N₆O₂•2H₂O: C 58.82, H 4.94, N 20.58; found: C 59.03, H 4.87, N 20.66.

 : It was synthesized in two steps from 5-bromo-2-methyl-pyridine using a reported method.¹

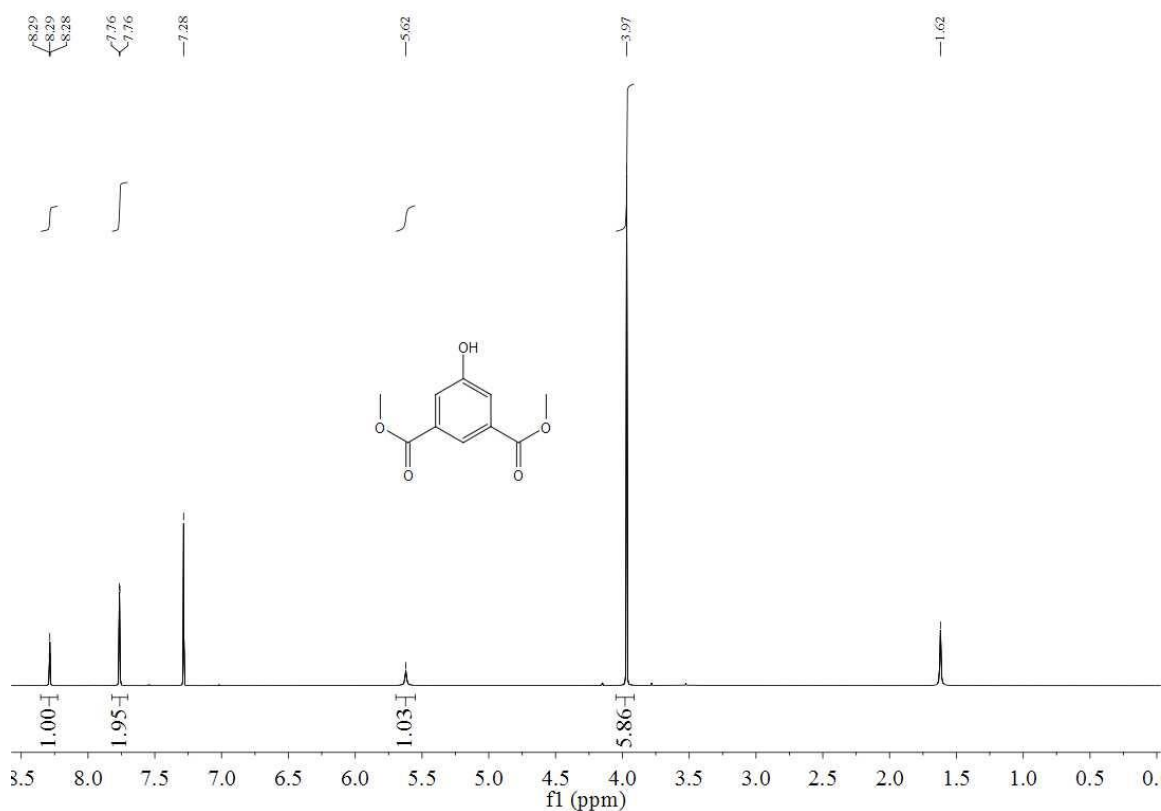


Figure S2. ¹H-NMR of 5-hydroxy-isophthalic acid dimethyl ester. Solvent: CDCl₃

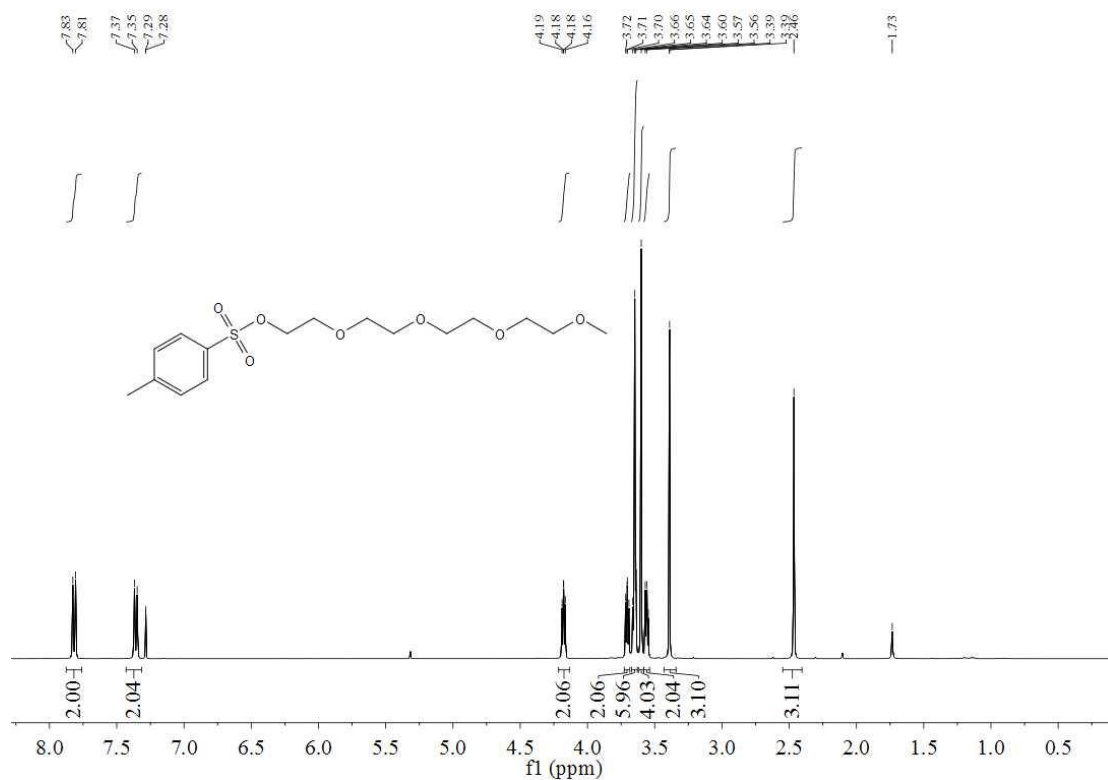


Figure S3. $^1\text{H-NMR}$ of toluene-4-sulfonic acid PEG ester. Solvent: CDCl_3

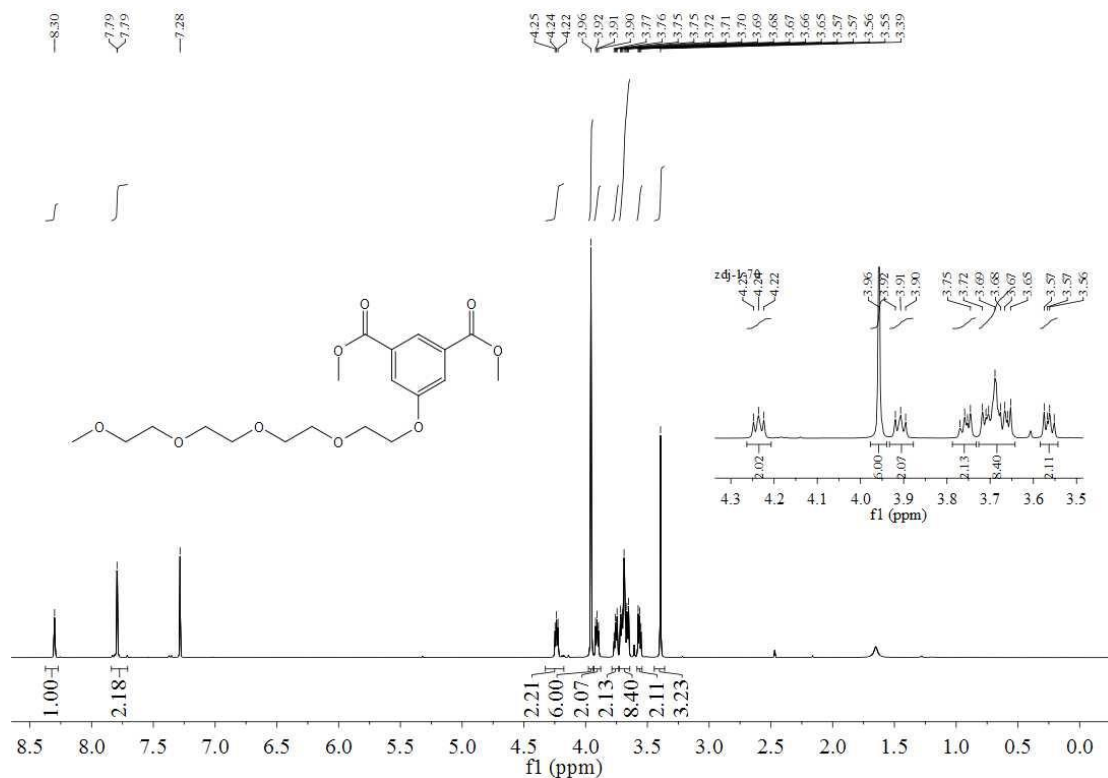


Figure S4. $^1\text{H-NMR}$ of 5-PEG-isophthalic acid dimethyl ester. Solvent: CDCl_3

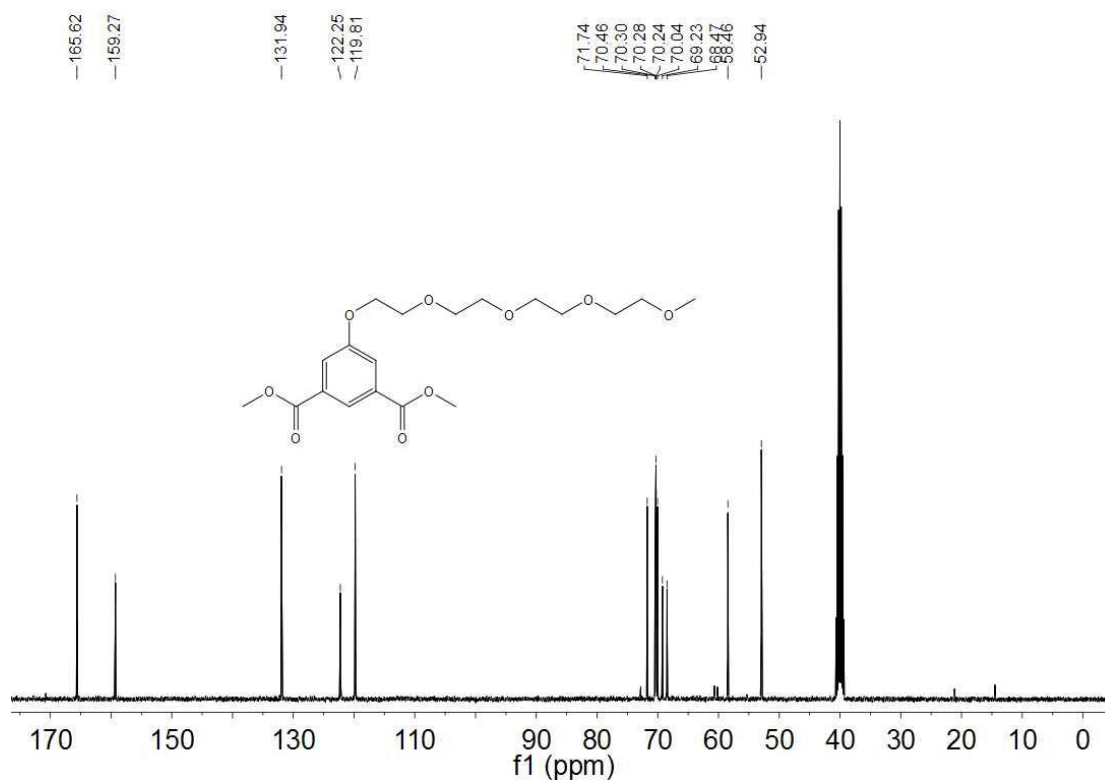


Figure S5. ^{13}C -NMR of 5-PEG-isophthalic acid dimethyl ester. Solvent: CDCl_3

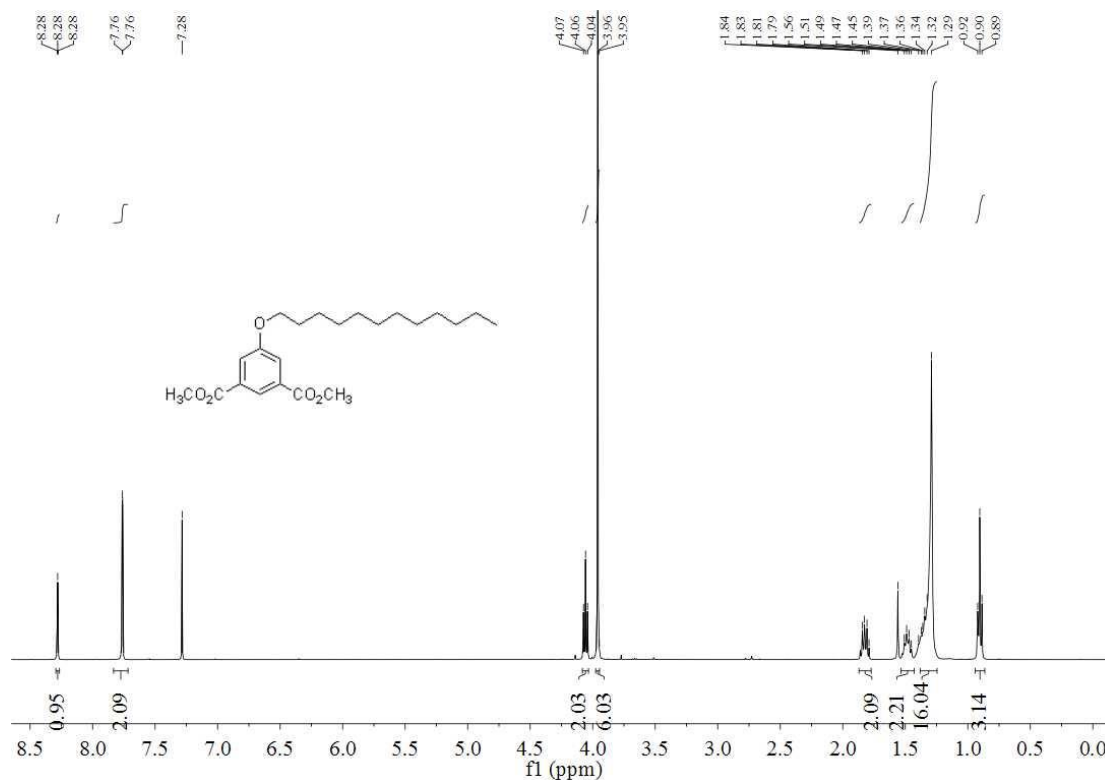


Figure S6. ^1H -NMR of 5-dodecyloxy-isophthalic acid dimethyl ester. Solvent: CDCl_3

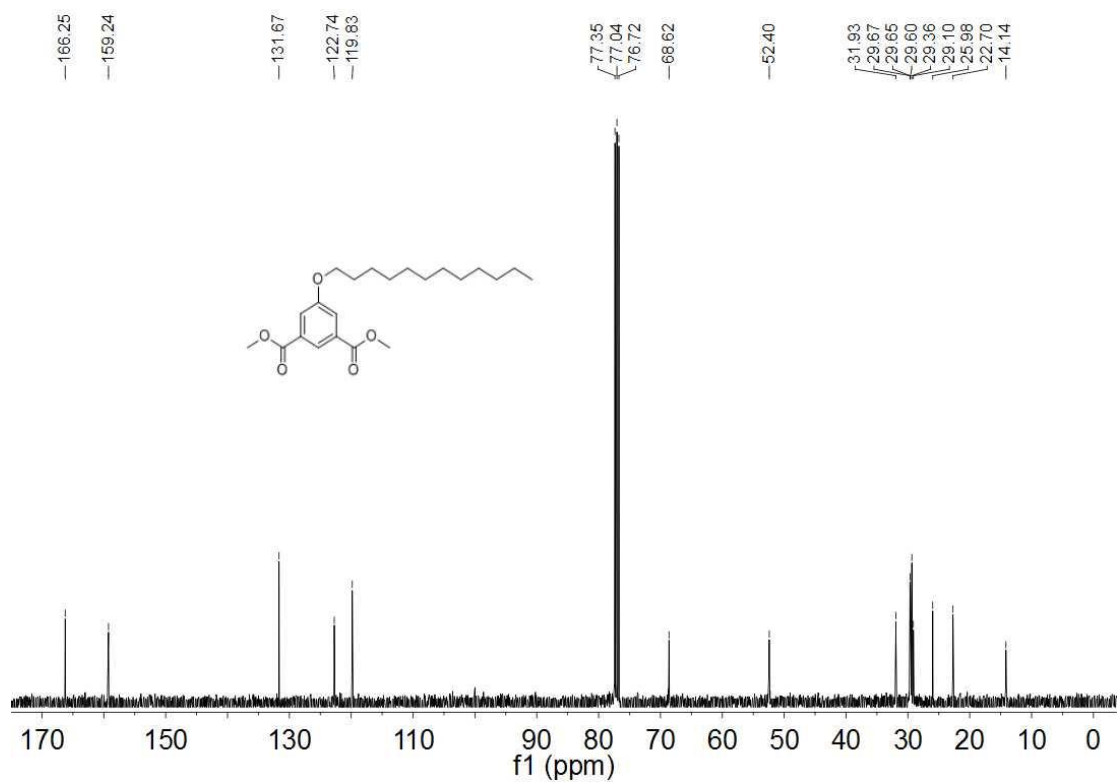


Figure S7. ^{13}C -NMR of 5-dodecyloxy-isophthalic acid dimethyl ester. Solvent: CDCl_3

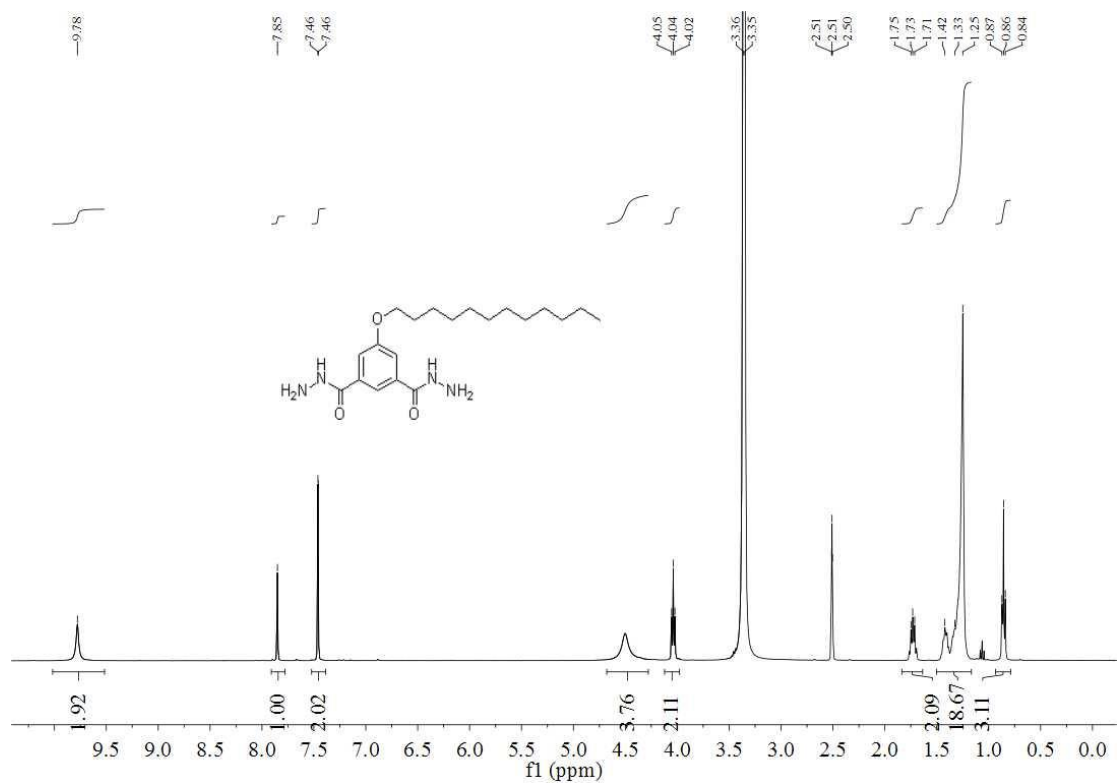


Figure S8. ^1H -NMR of 5-dodecyloxy-isophthalic dihydrazide. Solvent: DMSO-d_6

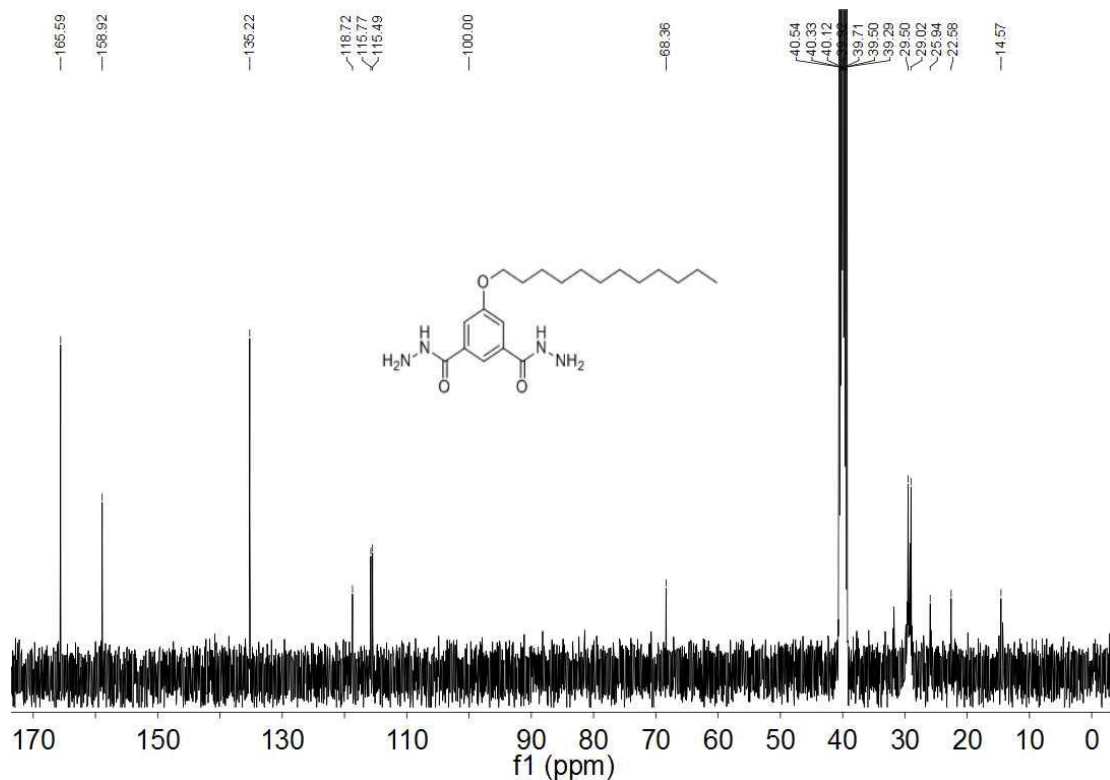


Figure S9. ¹³C-NMR of 5-dodecyloxy- isophthalic dihydrazide. Solvent: DMSO-d₆

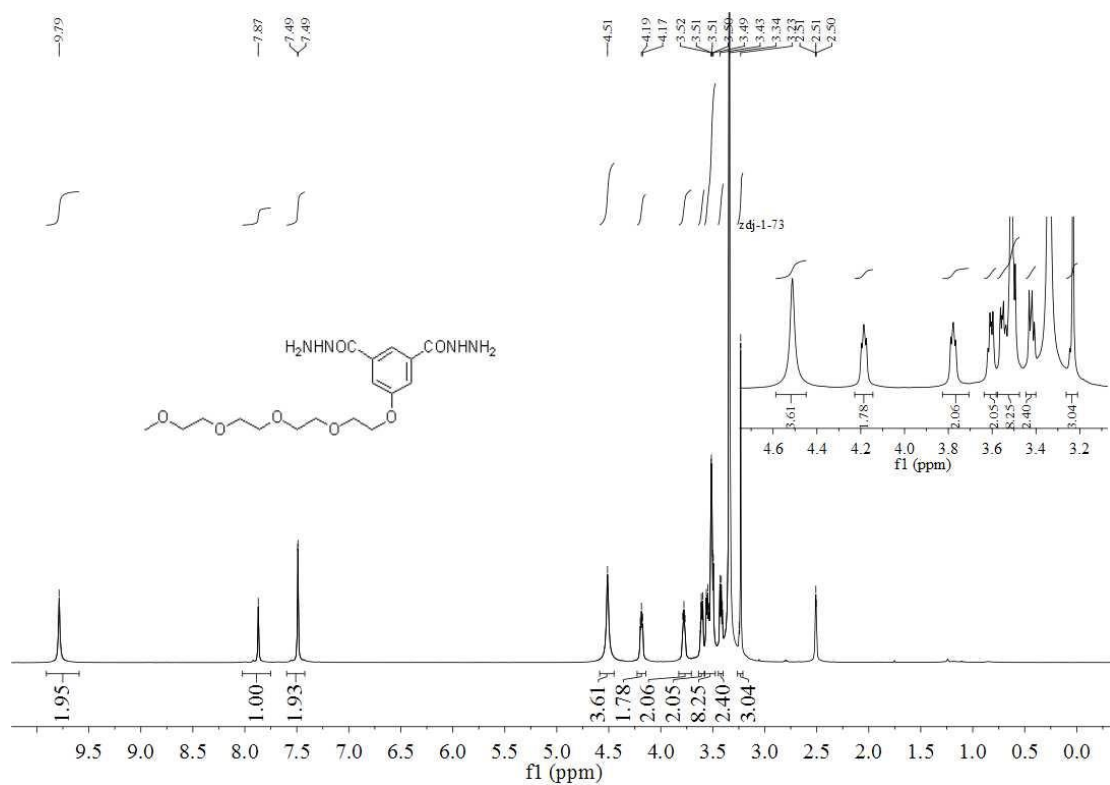


Figure S10. ¹H-NMR of 5-PEG- isophthalic dihydrazide. Solvent: DMSO-d₆

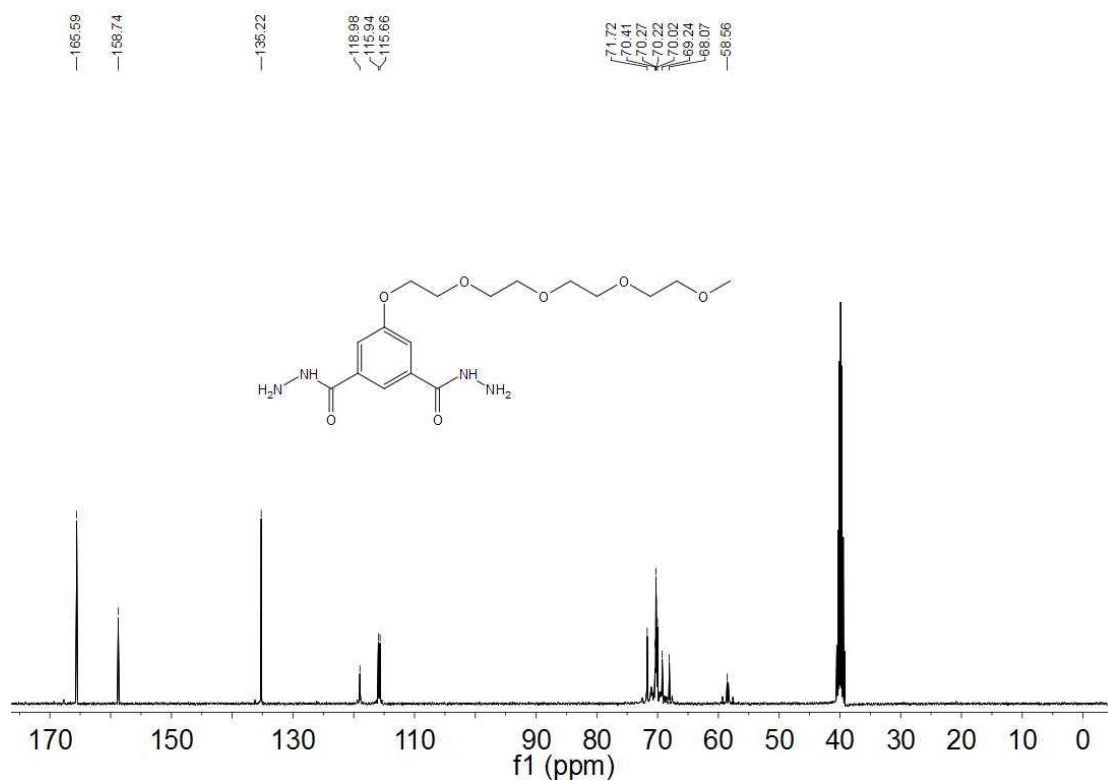


Figure S11. ^{13}C -NMR of 5-PEG- isophthalic dihydrazide. Solvent: DMSO-d_6

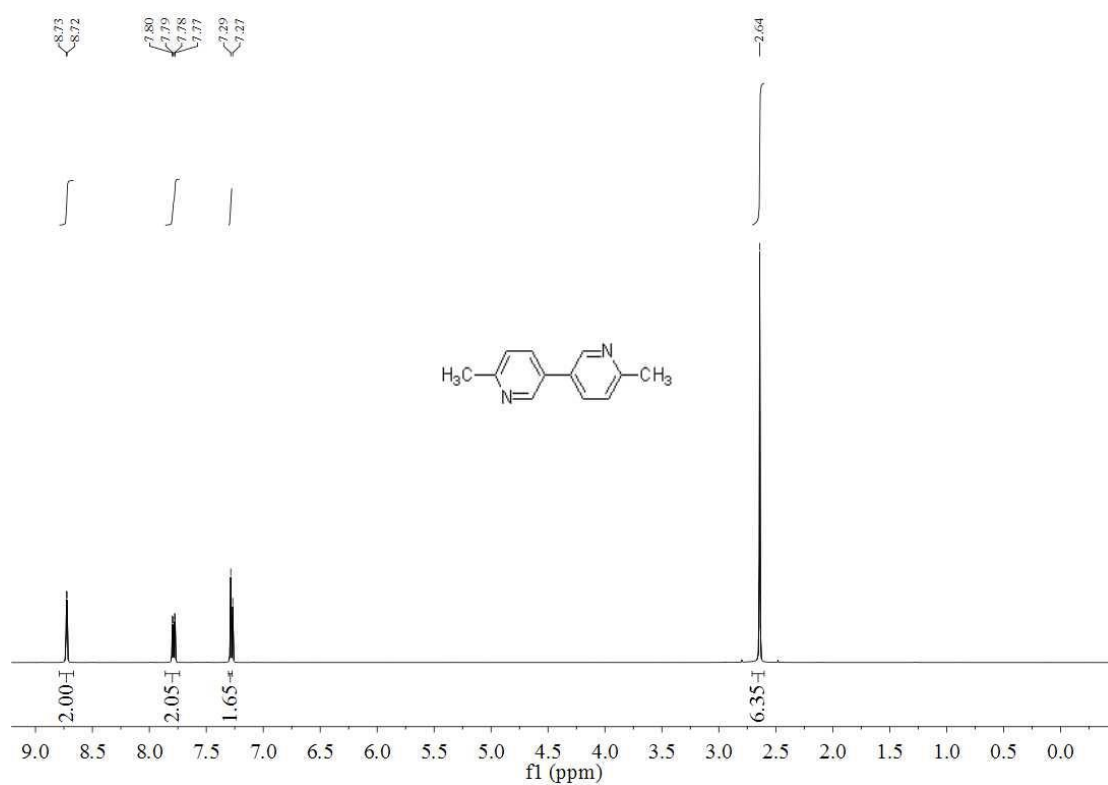


Figure S12. ^1H -NMR of 6,6'-dimethyl-3,3'-bipyridine. Solvent: CDCl_3

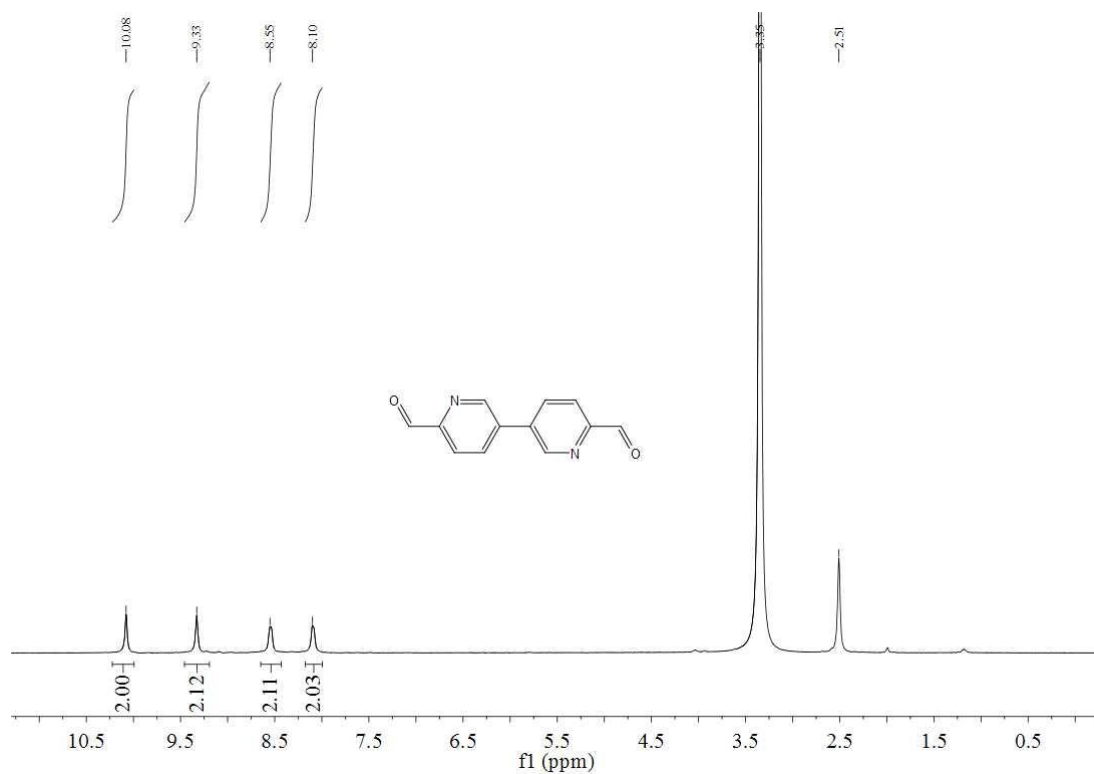


Figure S13. $^1\text{H-NMR}$ of 6,6'-diformyl-3,3'-bipyridine. Solvent: DMSO-d_6

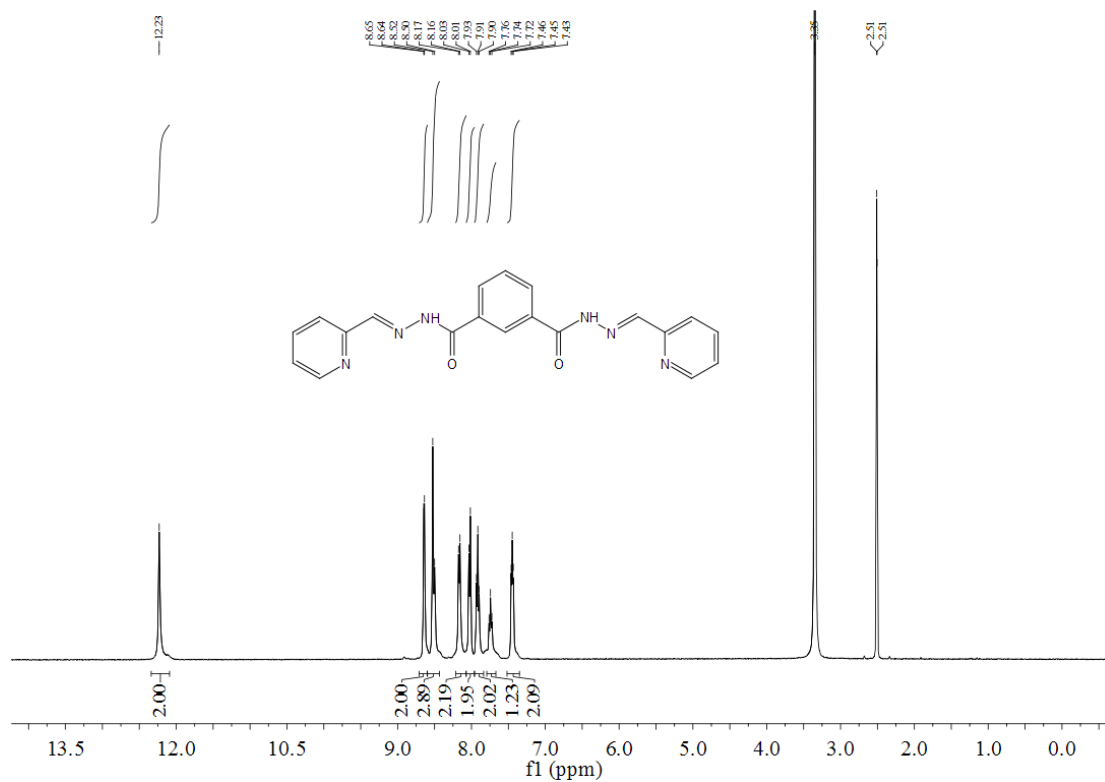


Figure S14. $^1\text{H-NMR}$ of the control compound **3**. Solvent: DMSO-d_6

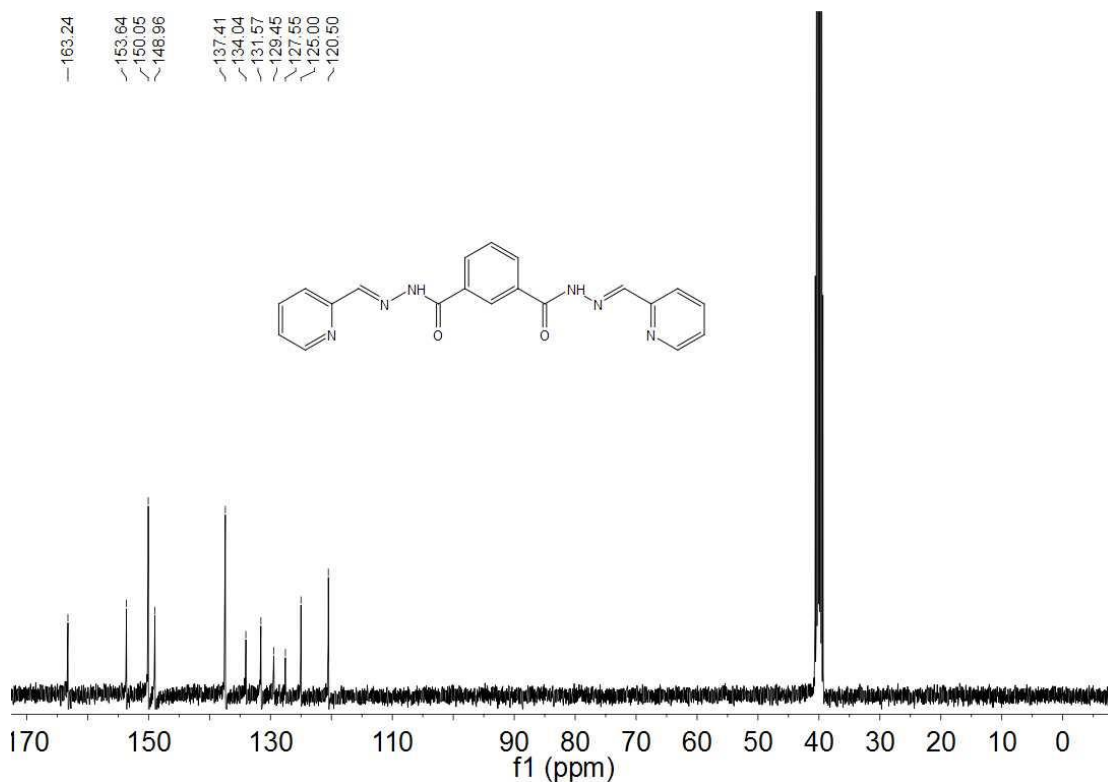


Figure S15. ¹³C-NMR of the control compound **3**. Solvent: DMSO-d₆

Preparation of dynamic covalent polymers

The dialdehyde and dihydrazide (the feed ratio is 1:1) were dissolved in methanol. Under inert atmosphere, the mixture solution was heated to 70 °C, and then stirred and refluxed at this temperature for 24 h. After cooling down to room temperature, the precipitate was filtered and washed with MeOH thoroughly. After dried under vacuum at room temperature, the dynamic covalent polymer containing the acylhydrazone bond was obtained.

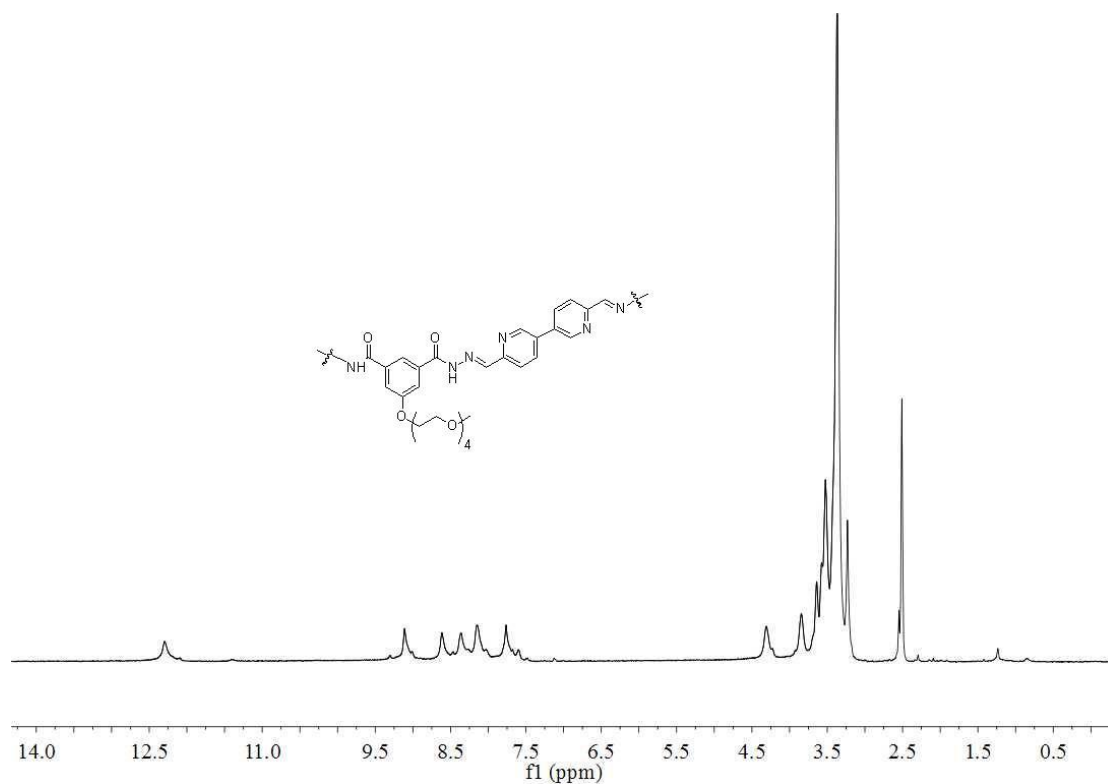


Figure S16. $^1\text{H-NMR}$ of the polymer **1**. Solvent: DMSO-d_6

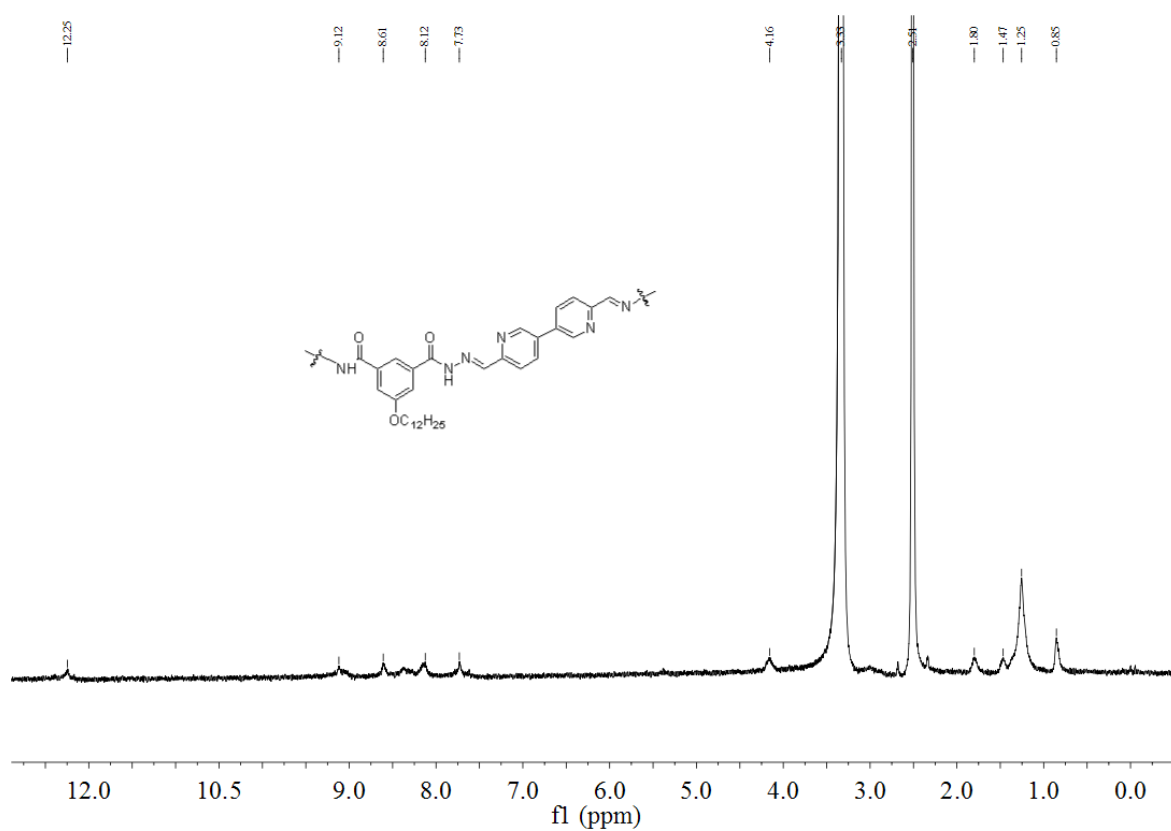


Figure S17. $^1\text{H-NMR}$ of the polymer **2**. Solvent: DMSO-d_6

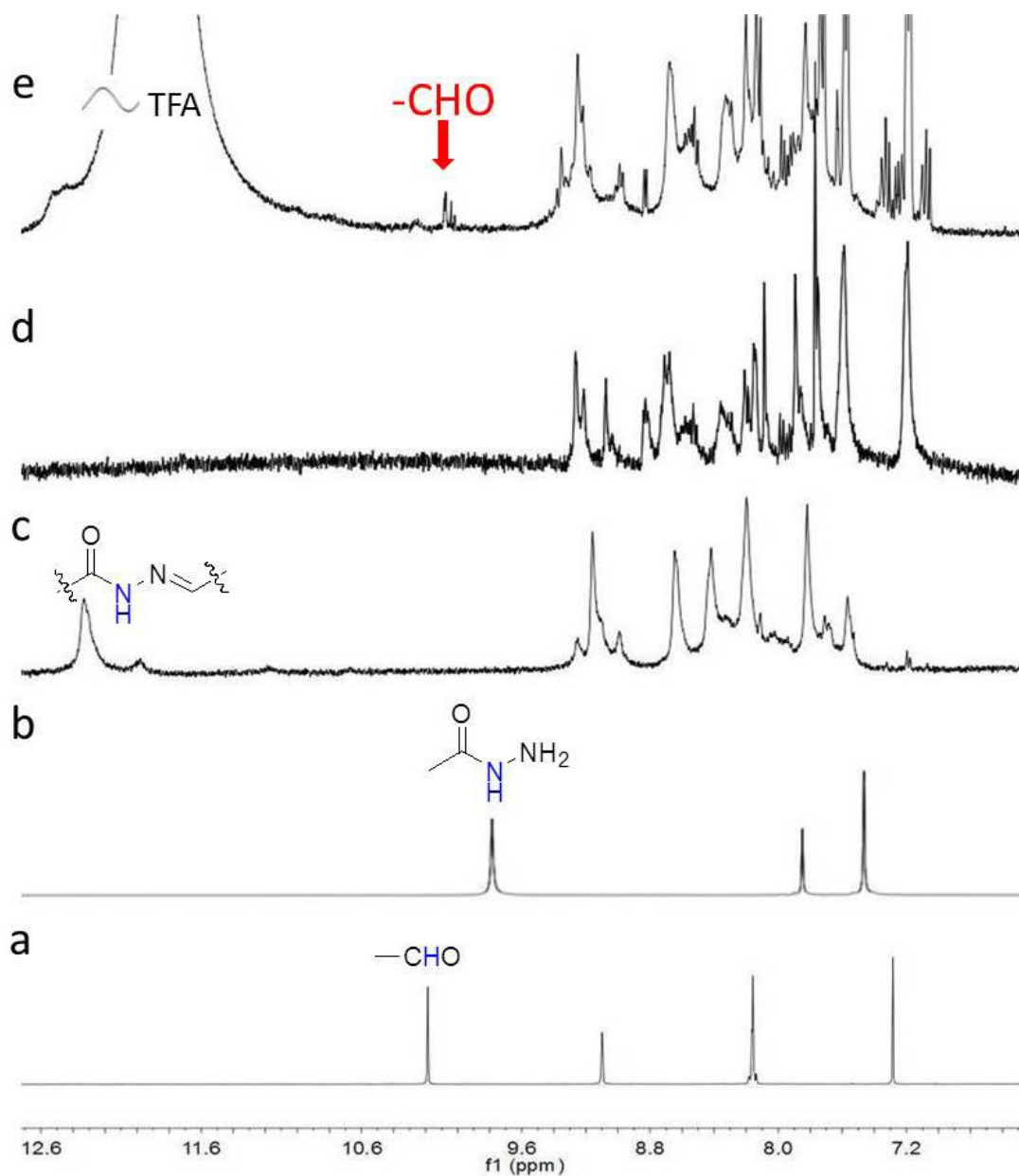


Figure S18. (a) $^1\text{H-NMR}$ of the monomer dialdehydes. (b) $^1\text{H-NMR}$ of the monomer dihydrazides. (c) $^1\text{H-NMR}$ of the polymer **1**. (d) $^1\text{H-NMR}$ of **1** with TFA. The concentration of TFA is 220 mM. (e) $^1\text{H-NMR}$ of **1** after heating at 110 $^\circ\text{C}$ for 24 h in the presence of TFA. The concentration of TFA is 220 mM. Solvent: DMSO-d_6

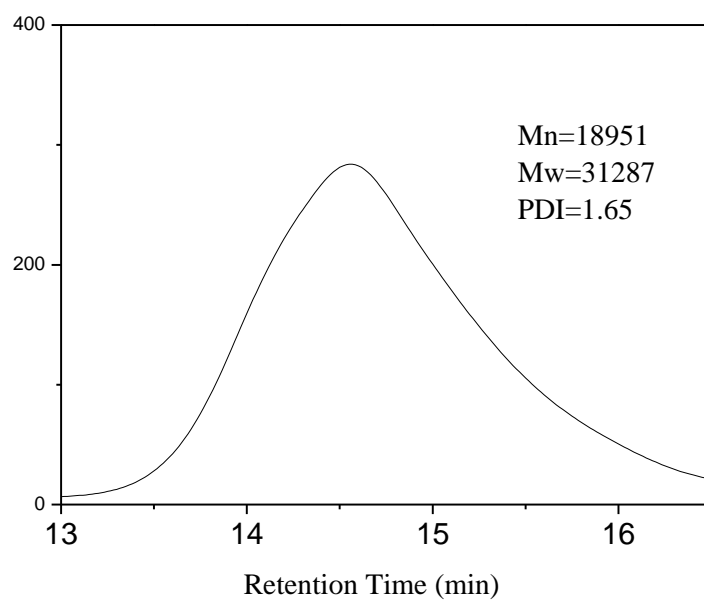


Figure S19. GPC data for polymer **1**

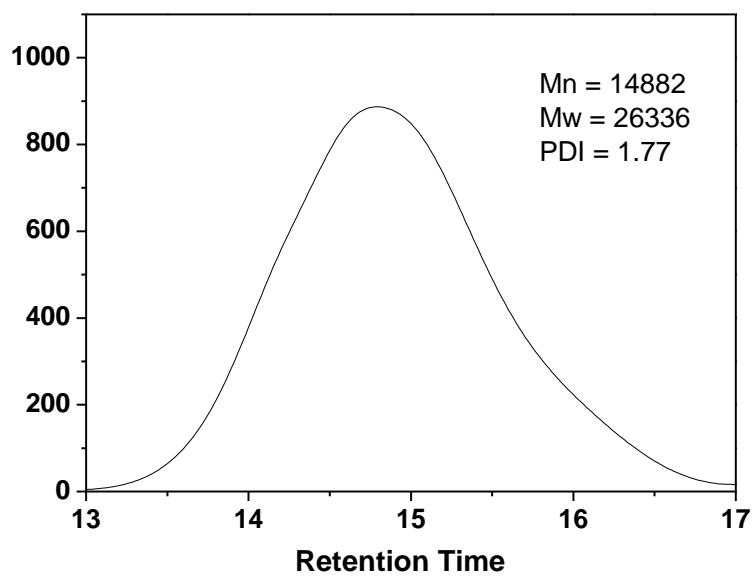


Figure S20. GPC data for polymer **2**

Stimuli responsiveness of dynamic covalent polymers

Polymer **1** in DMSO solution:

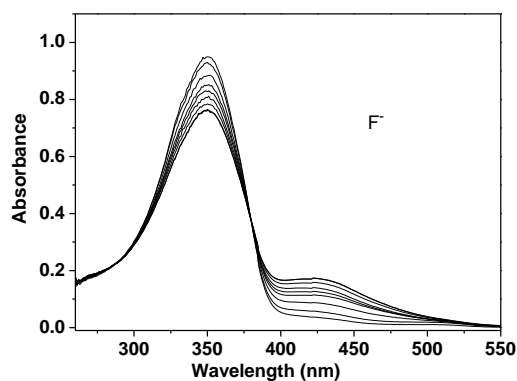


Figure S21. UV-vis absorption spectra of polymer **1** (15 µg/mL) with addition of various concentrations of Bu₄NF (0, 8.65, 17.26, 30.97, 44.58, 58.11, 74.89, 99.81, 132.57, and 164.8 µM, respectively) in 2.4 mL DMSO solution.

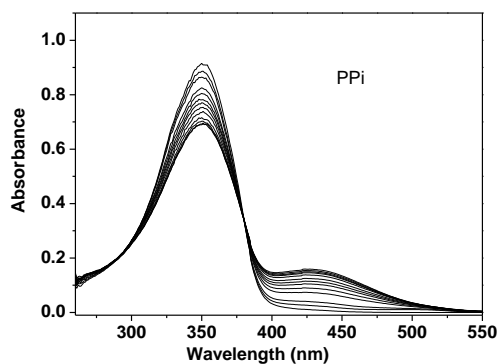


Figure S22. UV-vis absorption spectra of polymer **1** (15 µg/mL) with addition of various concentrations of PPI (0, 5.19, 13.82, 27.55, 41.19, 54.74, 71.55, 96.51, 129.32, 161.6, 193.37, and 224.64 µM, respectively) in 2.4 mL DMSO solution.

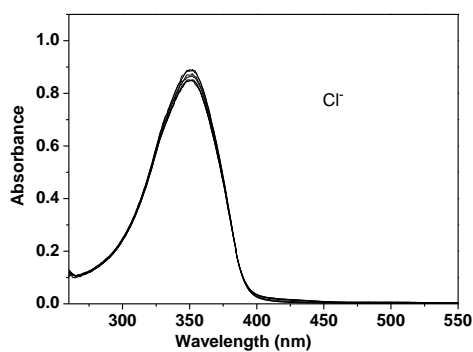


Figure S23. UV-vis absorption spectra of polymer **1** (15 µg/mL) with addition of various concentrations of Bu₄NCl (0, 8.64, 25.84, 51.36, 84.90, 117.89 and 454.74

μM , respectively) in 2.4 mL DMSO solution.

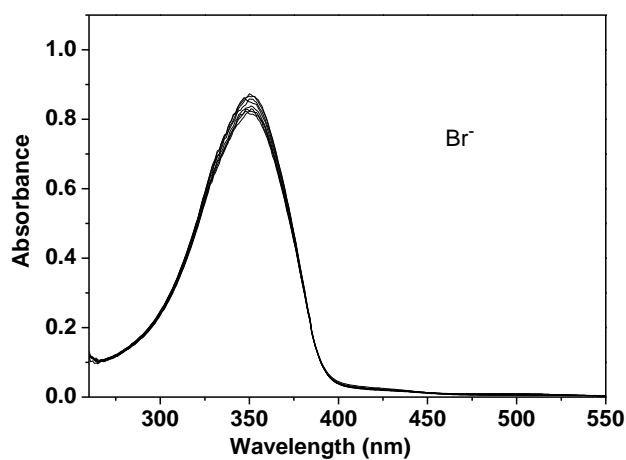


Figure S24. UV-vis absorption spectra of polymer **1** (15 $\mu\text{g/mL}$) with addition of various concentrations of Bu_4NBr (0, 8.64, 25.84, 51.36, 84.90, 117.89 and 454.74 μM , respectively) in 2.4 mL DMSO solution.

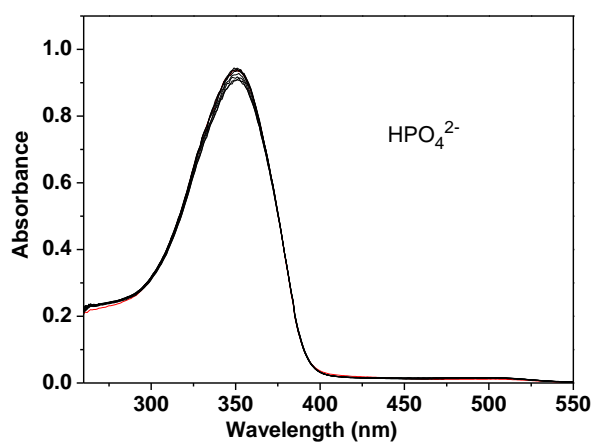


Figure S25. UV-vis absorption spectra of polymer **1** (15 $\mu\text{g/mL}$) with addition of various concentrations of $(\text{Bu}_4\text{N})_2\text{HPO}_4$ (0, 8.64, 25.84, 51.36, 84.90, 117.89 and 454.74 μM , respectively) in 2.4 mL DMSO solution.

Polymer **1** in DMSO: H₂O (4: 1 v/v) solution:

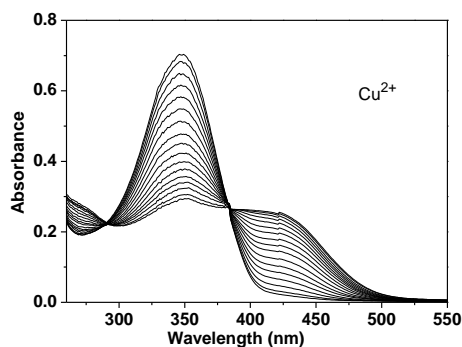


Figure S26. UV-vis absorption spectra of polymer **1** (12.2 μg/mL) with addition of various concentrations of Cu(OTf)₂ (0, 0.2162, 0.646, 1.0722, 1.7049, 2.3299, 2.9474, 3.759, 4.5578, 5.3439, 6.1176, 6.8794, 7.6293, 8.3678, 9.0951, 9.8113 and 10.5169 μM, respectively) in 2.4 mL DMSO: H₂O (4: 1 v/v) solution.

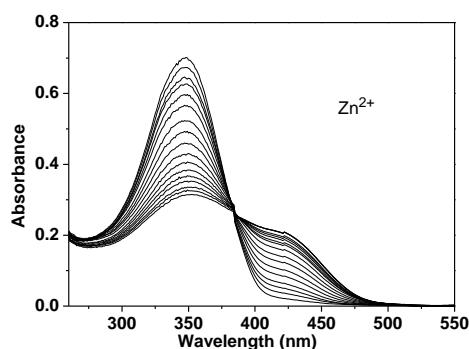


Figure S27. UV-vis absorption spectra of polymer **1** (12.2 μg/mL) with addition of various concentrations of Zn(OTf)₂ (0, 0.2162, 0.4315, 0.646, 1.0722, 1.4949, 2.1224, 2.7424, 3.5573, 4.3593, 5.1485, 5.9253, 6.6901, 7.4429 and 9.6333 μM, respectively) in 2.4 mL DMSO: H₂O (4: 1 v/v) solution.

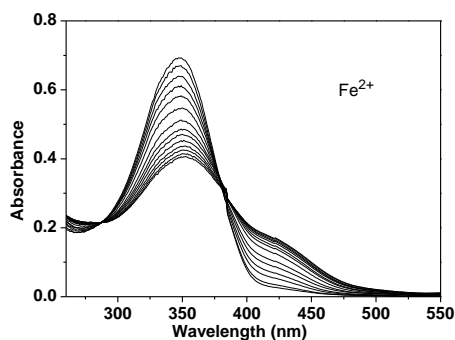


Figure S28. UV-vis absorption spectra of polymer **1** (12.2 μg/mL) with addition of various concentrations of Fe(ClO₄)₂ (0, 0.4315, 0.646, 1.0722, 1.7049, 2.3299, 3.1515, 3.9599, 4.7555, 5.5385, 6.3092, 7.068, 7.815 and 8.5507 μM, respectively) in 2.4 mL DMSO: H₂O (4: 1 v/v) solution.

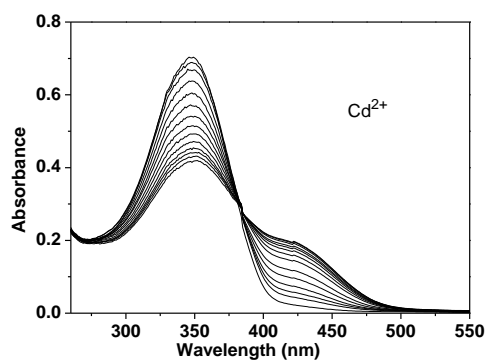


Figure S29. UV-vis absorption spectra of polymer **1** (12.2 $\mu\text{g/mL}$) with addition of various concentrations of $\text{Cd}(\text{ClO}_4)_2$ (0, 0.4315, 0.646, 1.0722, 1.7049, 2.3299, 3.1515, 3.9599, 4.7555, 5.5385, 6.3092, 7.068, 7.815 and 8.5507 μM , respectively) in 2.4 mL DMSO: H_2O (4: 1 v/v) solution.

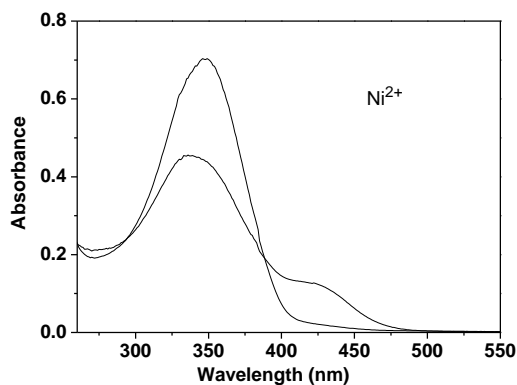


Figure S30. UV-vis absorption spectra of polymer **1** (12.2 $\mu\text{g/mL}$) with addition of various concentrations of $\text{Ni}(\text{ClO}_4)_2$ (0 and 9.8113 μM) in 2.4 mL DMSO: H_2O (4: 1 v/v) solution.

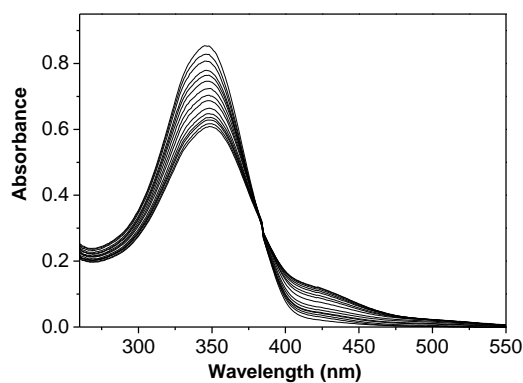


Figure S31. UV-vis absorption spectra of polymer **1** (12.5 $\mu\text{g/mL}$) with addition of

various concentrations of Bu₄NCN (0, 4.32, 12.42, 30.01, 60.03, 110.25, 250.31 and 432.16 μM, respectively) in 2.4 mL DMSO: H₂O (4: 1 v/v) solution.

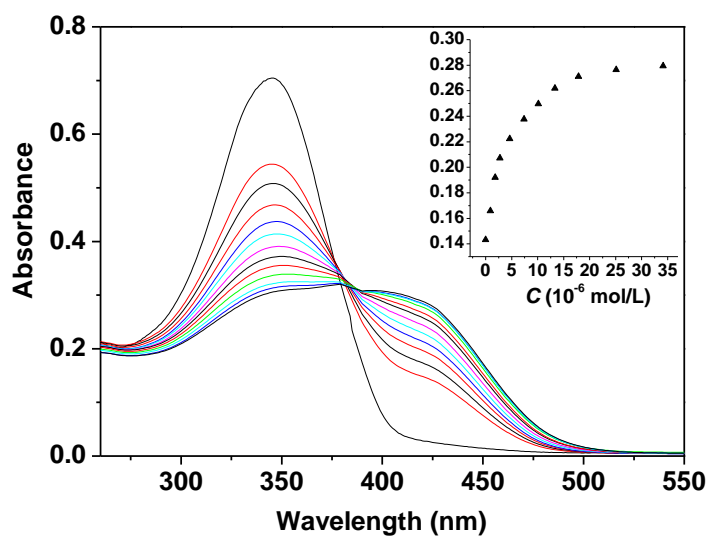


Figure S32. Spectral change and binding isotherm of polymer **1** (12 μg/mL) with Zn(OTf)₂ (18.5 μM) and various concentration of Bu₄NCN (0 to 325 μM) in 2.4 mL DMSO: H₂O (4: 1 v/v) solution.

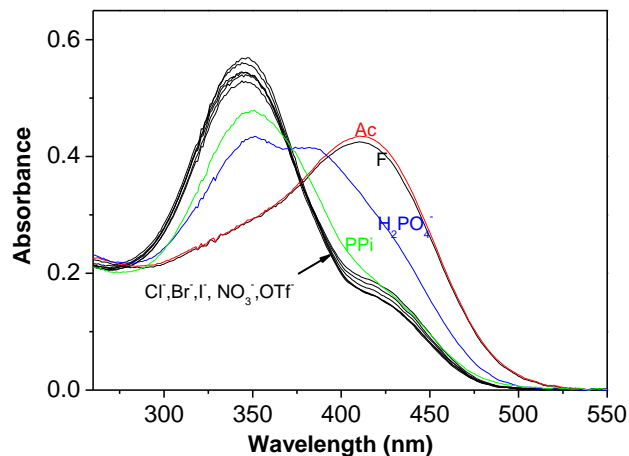


Figure S33. Cooperative binding studies: UV-vis spectra of **1** (12.2 μg/mL) with Zn(OTf)₂ (10 μM) and various salts of tetrabutylammonium (350 μM) in 4: 1 DMSO/H₂O.

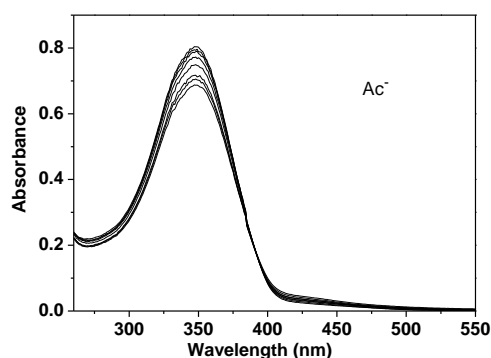


Figure S34. UV-vis absorption spectra of polymer **1** (12.2 μg/mL) with addition of various concentrations of Bu₄NAc (0, 8.64, 25.84, 59.79, 126.06, 221.538, 545.44 and 864.31 μM, respectively) in 2.4 mL DMSO: H₂O (4: 1 v/v) solution.

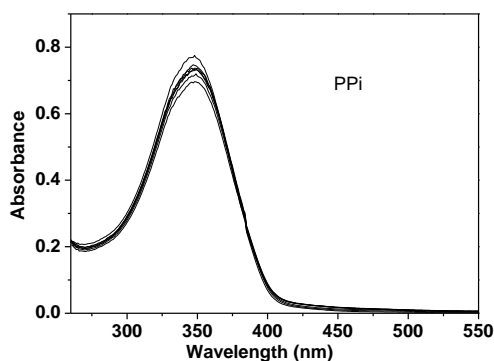


Figure S35. UV-vis absorption spectra of polymer **1** (12.2 μg/mL) with addition of various concentrations of PPI (0, 8.64, 25.84, 59.79, 126.06, 221.538, 545.44 and 864.31 μM, respectively) in 2.4 mL DMSO: H₂O (4: 1 v/v) solution.

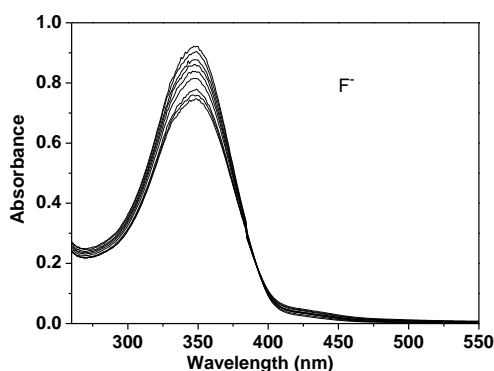


Figure S36. UV-vis absorption spectra of polymer **1** (15 μg/mL) with addition of various concentrations of Bu₄NF (0, 8.64, 25.84, 59.79, 126.06, 221.538, 545.44 and 864.31 μM, respectively) in 2.4 mL DMSO: H₂O (4: 1 v/v) solution.

Polymer **1** in DMSO: H₂O (1: 1 v/v) solution:

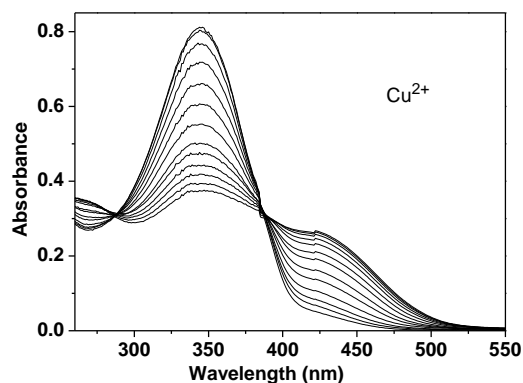


Figure S37. UV-vis absorption spectra of polymer **1** (15 µg/mL) with addition of various concentrations of Cu(OTf)₂ (0, 0.8595, 1.7049, 2.9474, 4.16, 5.7323, 7.2558, 8.7328, 10.1654, 11.5556, 12.9051 and 14.2158 µM, respectively) in 2.4 mL DMSO: H₂O (1: 1 v/v) solution.

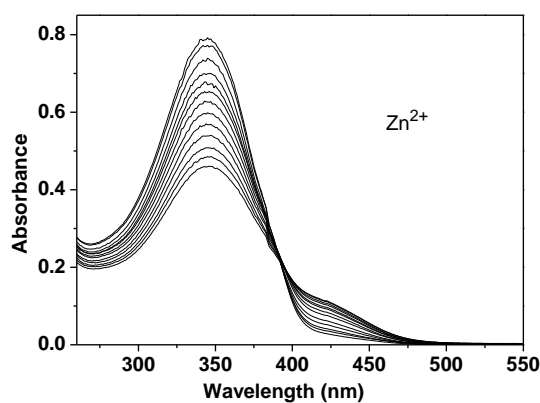


Figure S38. UV-vis absorption spectra of polymer **1** (15 µg/mL) with addition of various concentrations of Zn(OTf)₂ (0, 0.2162, 0.646, 1.4949, 2.3299, 3.9599, 5.5385, 7.815, 9.9887, 12.4037, 15.016, 17.4835 and 19.8179 µM, respectively) in 2.4 mL DMSO: H₂O (1: 1 v/v) solution.

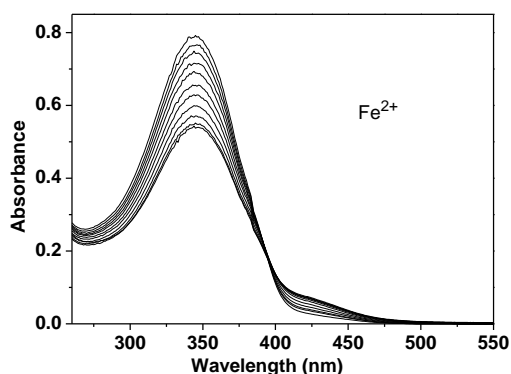


Figure S39. UV-vis absorption spectra of polymer **1** (15 µg/mL) with addition of various concentrations of $\text{Fe}(\text{ClO}_4)_2$ (0, 0.4315, 0.8595, 1.7049, 2.9474, 4.5578, 6.5, 8.7328, 11.2119 and 13.8917 µM, respectively) in 2.4 mL DMSO: H_2O (1: 1 v/v) solution.

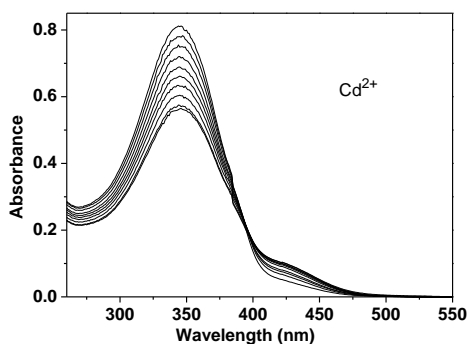


Figure S40. UV-vis absorption spectra of polymer **1** (15 µg/mL) with addition of various concentrations of $\text{Cd}(\text{ClO}_4)_2$ (0, 0.4315, 1.284, 2.1224, 3.759, 5.3439, 7.6293, 10.5169 and 13.2364 µM, respectively) in 2.4 mL DMSO: H_2O (1: 1 v/v) solution.

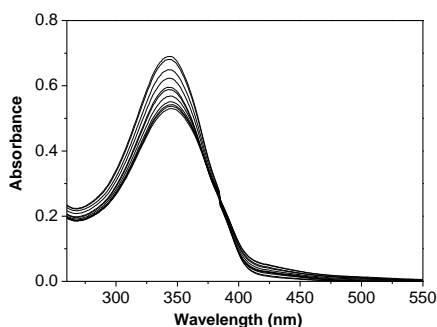


Figure S41. UV-vis absorption spectra of polymer **1** (15 µg/mL) with addition of various concentrations of Bu_4NCN (0, 6.78, 18.31, 40.06, 84.46, 148.63, 365.45 and 579.08 µM, respectively) in 2.4 mL DMSO: H_2O (4: 1 v/v) solution.

Polymer **1** in H₂O solution:

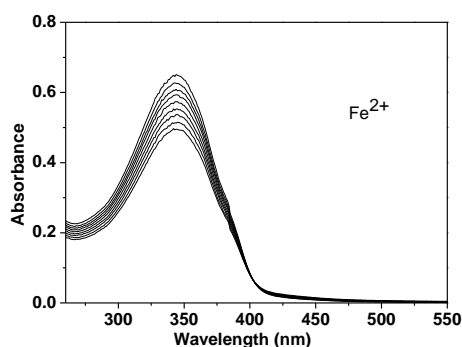


Figure S42. UV-vis absorption spectra of polymer **1** (13 µg/mL) with addition of various concentrations of Fe(ClO₄)₂ (0, 0.4315, 1.284, 2.536, 4.16, 6.1176, 8, 10.5168 and 13.8363 µM, respectively) in 2.4 mL H₂O solution.

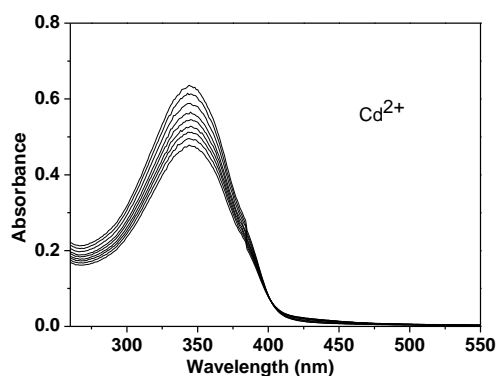


Figure S43. UV-vis absorption spectra of polymer **1** (13 µg/mL) with addition of various concentrations of Cd(ClO₄)₂ (0, 0.4315, 1.284, 2.536, 4.16, 6.1176, 8, 10.5168 and 13.8363 µM, respectively) in 2.4 mL H₂O solution.

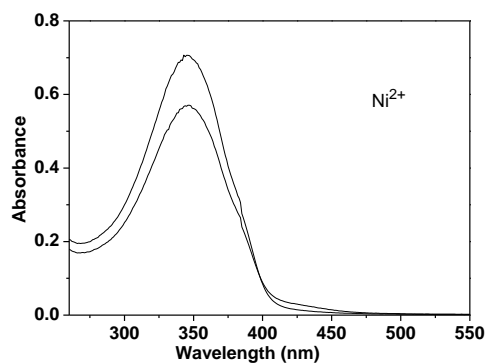


Figure S44. UV-vis absorption spectra of polymer **1** (13 µg/mL) with addition of various concentrations of Ni(ClO₄)₂ (0 and 13.8363 µM) in 2.4 mL H₂O solution.

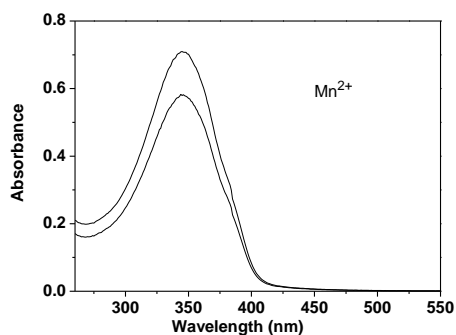


Figure S45. UV-vis absorption spectra of polymer **1** (13 µg/mL) with addition of various concentrations of $\text{Mn}(\text{ClO}_4)_2$ (0 and 13.8363 µM) in 2.4 mL H_2O solution.

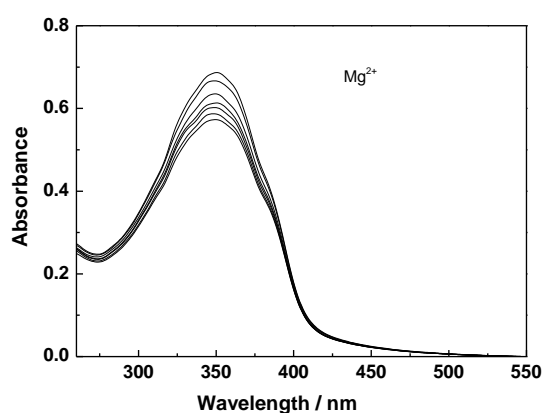


Figure S46. UV-vis absorption spectra of polymer **1** (13 µg/mL) with addition of various concentrations of $\text{Mg}(\text{ClO}_4)_2$ (0, 1.309, 5.206, 11.50, 20.16, 100.78, and 224.55 µM, respectively) in 2.4 mL H_2O solution.

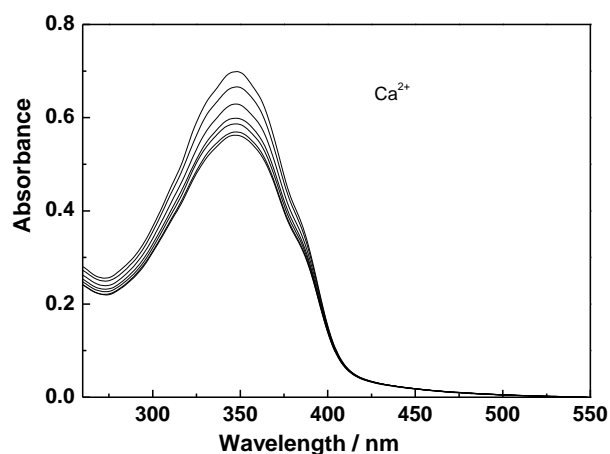


Figure S47. UV-vis absorption spectra of polymer **1** (13 µg/mL) with addition of various concentrations of $\text{Ca}(\text{ClO}_4)_2$ (0, 2.051, 8.154, 18.159, 31.82, 110.15, and 200.37 µM, respectively) in 2.4 mL H_2O solution.

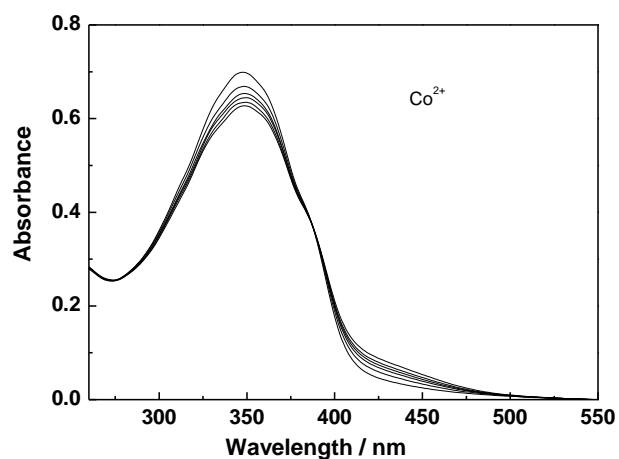


Figure S48. UV-vis absorption spectra of polymer **1** (13 $\mu\text{g/mL}$) with addition of various concentrations of $\text{Co}(\text{ClO}_4)_2$ (0, 1.185, 2.365, 4.710, 10.489, 18.383, 98.76 and 196.43 μM , respectively) in 2.4 mL H_2O solution.

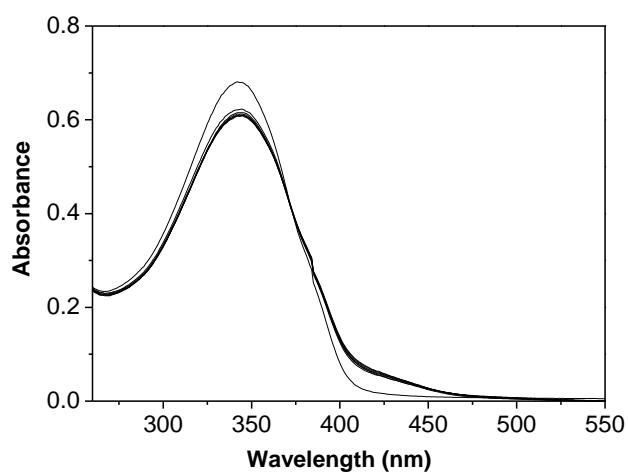


Figure S49. UV-vis absorption spectra of polymer **1** (13 $\mu\text{g/mL}$) with addition of various concentrations of Bu_4NCN (0, 310.25 and 430 μM) in 2.4 mL H_2O solution.

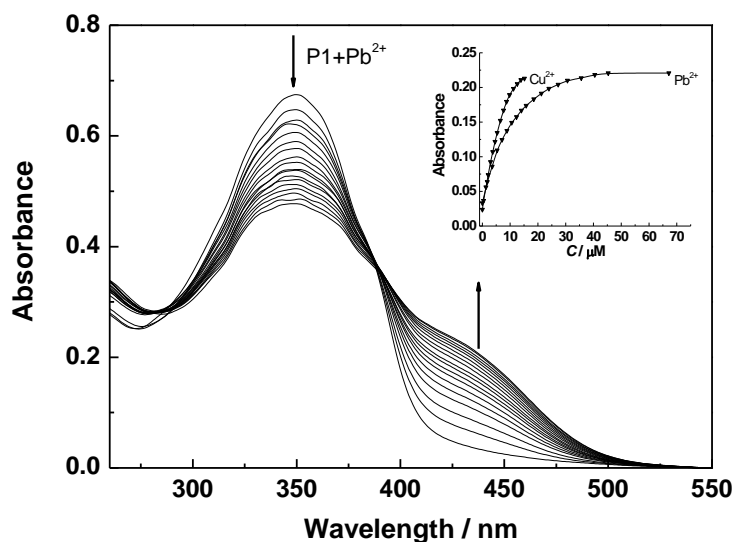


Figure S50. UV-vis absorption spectra of polymer **1** (13 µg/mL) with addition of various concentrations of $\text{Pb}(\text{ClO}_4)_2$ (0, 1.782, 3.556, 5.323, 7.083, 8.835, 10.58, 12.32, 14.05, 15.77, 18.52, 21.24, 23.95, 27.31, 30.64, 35.59, 40.48, 45.32 and 67.14 µM, respectively) in 2.4 mL H_2O solution.

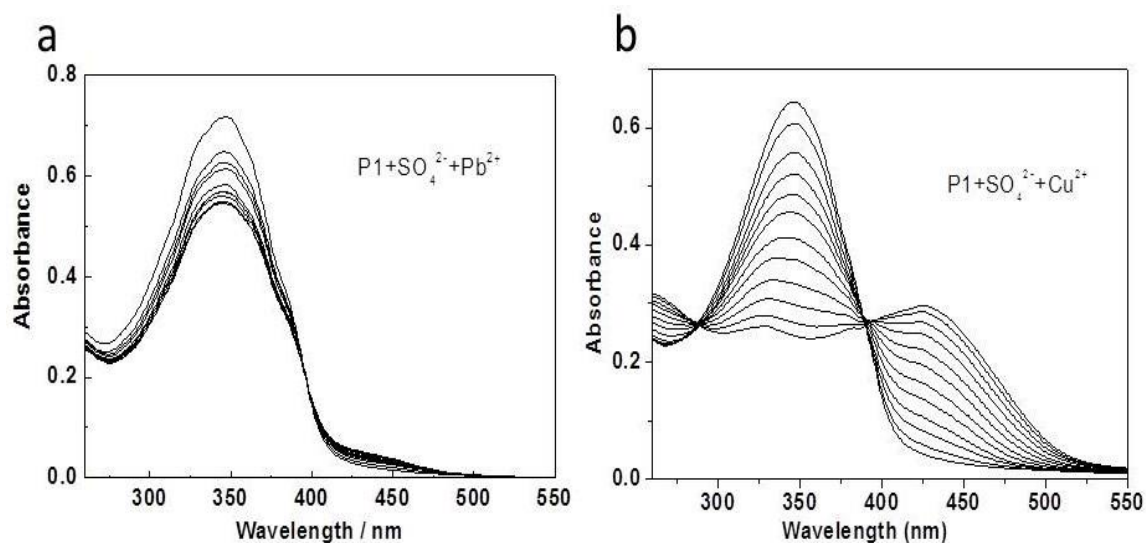


Figure S51. (a) UV-vis absorption spectra of polymer **1** (13 µg/mL) in the presence of Na_2SO_4 (100 µM) with addition of various concentrations of $\text{Pb}(\text{ClO}_4)_2$ (0 to 100 µM, respectively) in 2.4 mL H_2O solution. (b) UV-vis absorption spectra of polymer **1** (13 µg/mL) with addition of various concentrations of CuSO_4 (0 to 16 µM, respectively) in 2.4 mL H_2O solution.

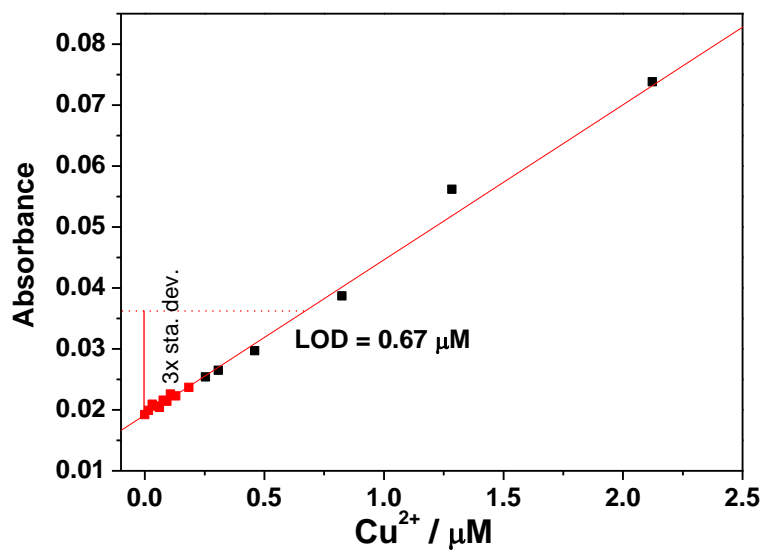


Figure S52. A regression line was fitted to the linear portion of the response curve, and the limit of detection was calculated considering 3x the standard deviation associate with repeated measurements of the aqueous solution of **1** in the absence of Cu^{2+} .

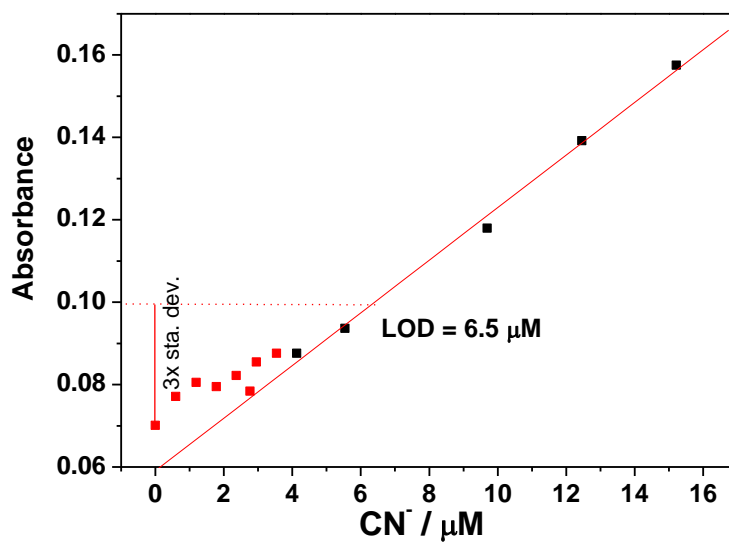


Figure S53. A regression line was fitted to the linear portion of the response curve, and the limit of detection was calculated considering 3x the standard deviation associate with repeated measurements of the aqueous solution of **1** in the absence of CN^- . 18.5 μM $\text{Zn}(\text{OTf})_2$ was in the solution for all the measurement.

Polymer 1 in PBS buffer:

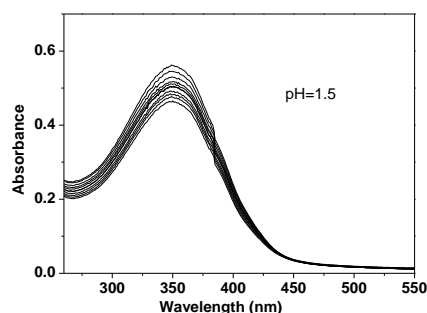


Figure S54. UV-vis absorption spectra of polymer **1** (13 $\mu\text{g}/\text{mL}$) with addition of various concentrations of $\text{Cu}(\text{OTf})_2$ (0, 0.4315, 1.2838, 2.9473, 4.5578, 6.8793, 9.095 and 11.2119 μM , respectively) in 2.4 mL PBS buffer (pH = 1.5) solution.

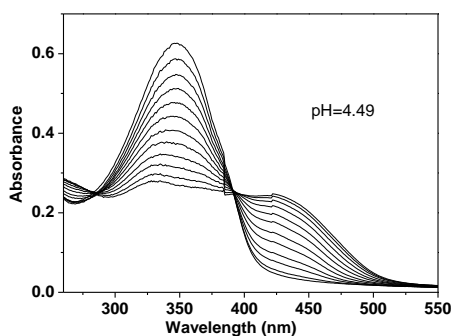


Figure S55. UV-vis absorption spectra of polymer **1** (13 $\mu\text{g}/\text{mL}$) with addition of various concentrations of $\text{Cu}(\text{OTf})_2$ (0, 0.4315, 1.284, 2.1224, 3.3548, 4.5578, 6.1176, 7.6293, 9.4545, 11.2119, 13.2364 and 16.1127 μM , respectively) in 2.4 mL PBS buffer (pH = 4.49) solution.

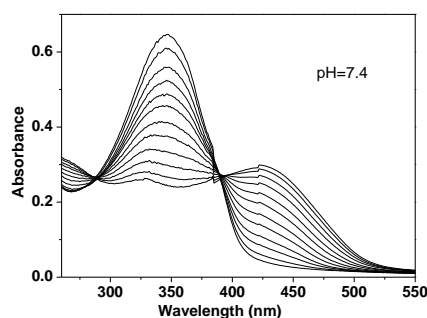


Figure S56. UV-vis absorption spectra of polymer **1** (13 $\mu\text{g}/\text{mL}$) with addition of various concentrations of $\text{Cu}(\text{OTf})_2$ (0, 0.4315, 1.284, 2.1224, 3.3548, 4.5578, 6.1176, 7.6293, 9.4545, 11.2119, 13.2364 and 16.1127 μM , respectively) in 2.4 mL PBS buffer (pH = 7.4) solution.

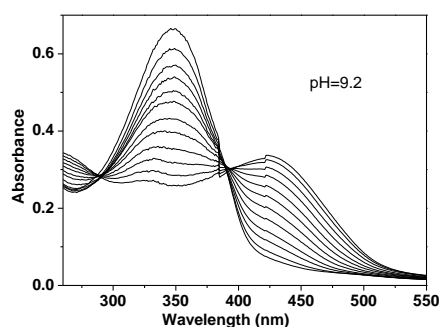


Figure S57. UV-vis absorption spectra of polymer **1** (13 µg/mL) with addition of various concentrations of Cu(OTf)₂ (0, 0.4315, 1.284, 2.1224, 3.3548, 4.5578, 6.1176, 7.6293, 9.4545, 11.2119, 13.2364 and 16.1127 µM, respectively) in 2.4 mL PBS buffer (pH = 9.2) solution.

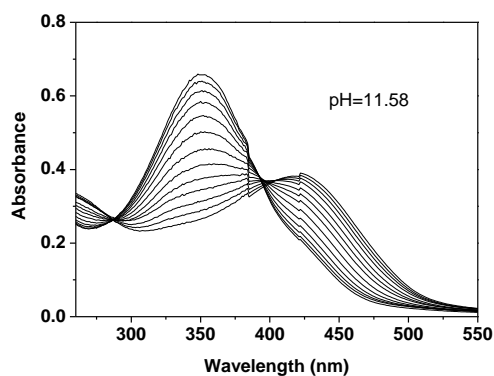


Figure S58. UV-vis absorption spectra of polymer **1** (13 µg/mL) with addition of various concentrations of Cu(OTf)₂ (0, 0.4315, 1.2838, 2.5366, 4.16, 6.1176, 8.3678, 10.5168, 12.5714, 14.5376, 16.4210, 18.226 and 19.9595 µM, respectively) in 2.4 mL PBS buffer (pH = 11.58) solution.

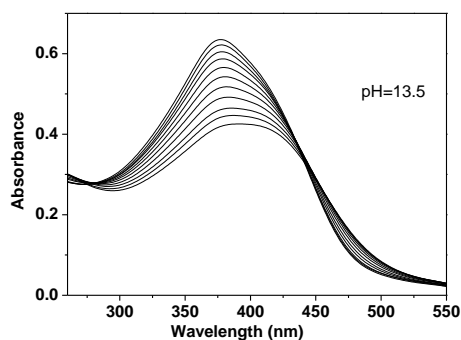


Figure S59. UV-vis absorption spectra of polymer **1** (13 µg/mL) with addition of various concentrations of Cu(OTf)₂ (0, 0.4315, 1.2838, 2.5366, 4.16, 6.1176, 8.3678, 10.8656, 13.5652, 16.1127 and 18.520 µM, respectively) in 2.4 mL PBS buffer (pH = 13.5) solution.

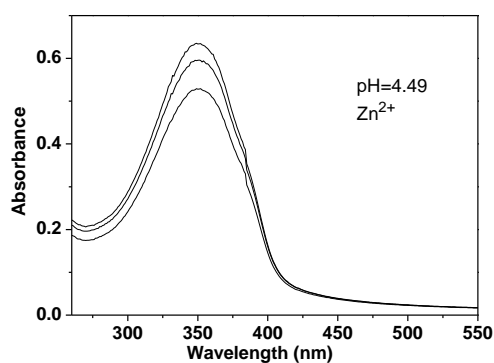


Figure S60. UV-vis absorption spectra of polymer **1** (13 $\mu\text{g/mL}$) with addition of various concentrations of $\text{Zn}(\text{OTf})_2$ (0, 2.5366 and 13.5652 μM , respectively) in 2.4 mL PBS buffer (pH = 4.49) solution.

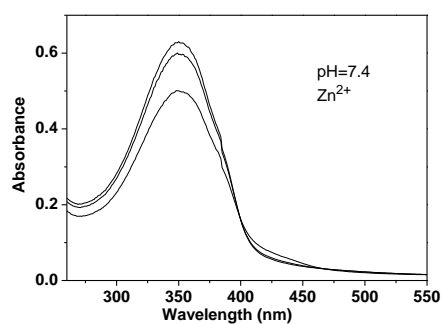


Figure S61. UV-vis absorption spectra of polymer **1** (13 $\mu\text{g/mL}$) with addition of various concentrations of $\text{Zn}(\text{OTf})_2$ (0, 2.5366 and 13.5652 μM , respectively) in 2.4 mL PBS buffer (pH = 7.4) solution.

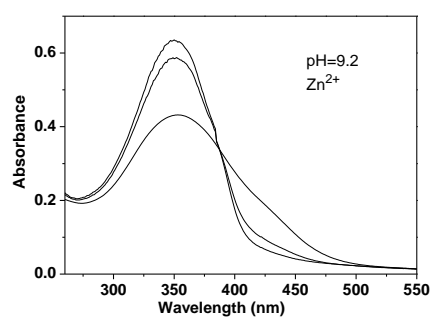


Figure S62. UV-vis absorption spectra of polymer **1** (13 $\mu\text{g/mL}$) with addition of various concentrations of $\text{Zn}(\text{OTf})_2$ (0, 2.5366 and 13.5652 μM , respectively) in 2.4 mL PBS buffer (pH = 9.2) solution.

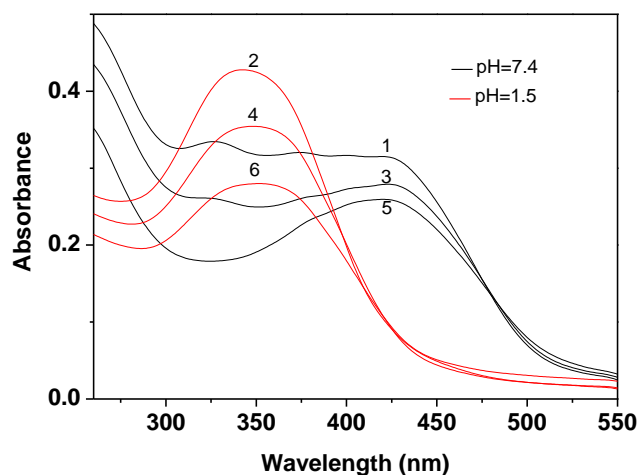


Figure S63. UV-vis absorption of polymer **1** (20 $\mu\text{g}/\text{mL}$) and $\text{Cu}(\text{OTf})_2$ (15 μmol) solution at $\text{pH}=7.4$ (black line), which is then acidified to $\text{pH}=1.5$ (red line). The pH was switched between 1.5 and 7.4. The decrease in absorbance at pH 1.5 (spectra 2, 4 and 6) or pH 7.4 (spectra 1, 3 and 5) is due to dilution.

Polymer **2** in DMSO solution:

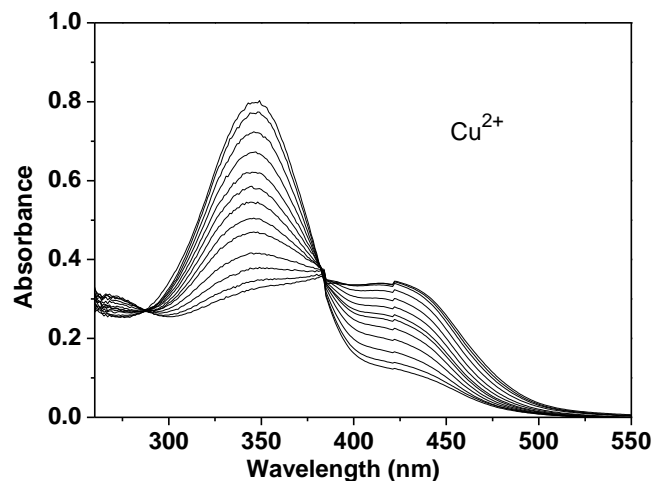


Figure S64. UV-vis absorption spectra of polymer **2** (13 $\mu\text{g}/\text{mL}$) with addition of various concentrations of $\text{Cu}(\text{OTf})_2$ (0, 0.8595, 1.7049, 2.5366, 3.3548, 4.16, 4.9524, 6.1176, 7.2558, 8.7328, 10.1654 and 11.5555 μM , respectively) in 2.4 mL DMSO solution.

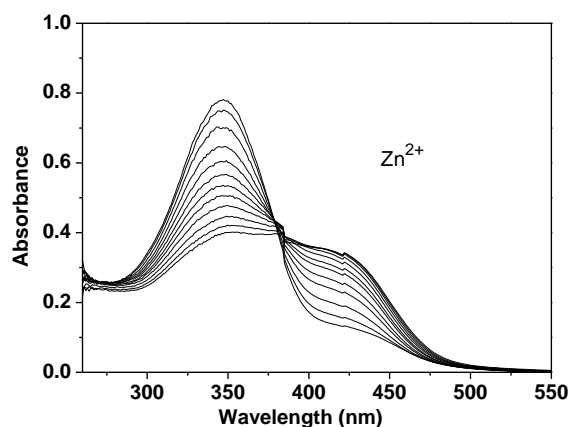


Figure S65. UV-vis absorption spectra of polymer **2** (13 µg/mL) with addition of various concentrations of Zn(OTf)₂ (0, 0.8595, 1.7049, 2.5366, 3.3548, 4.16, 4.9524, 6.1176, 7.2558, 8.7328, 10.1654 and 11.5555 µM, respectively) in 2.4 mL DMSO solution.

Polymer **2** in DMSO: H₂O (4: 1 v/v) solution:

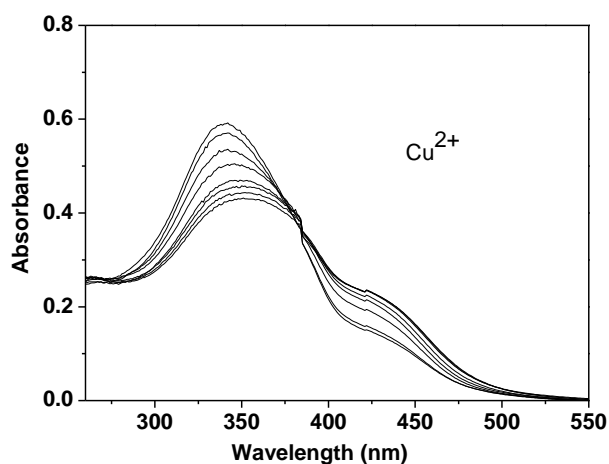


Figure S66. UV-vis absorption spectra of polymer **2** (13 µg/mL) with addition of various concentrations of Cu(OTf)₂ (0, 0.8595, 1.7049, 2.5366, 3.7590, 4.9524, 6.5, 8 and 9.4545 µM, respectively) in 2.4 mL DMSO: H₂O (4: 1 v/v) solution.

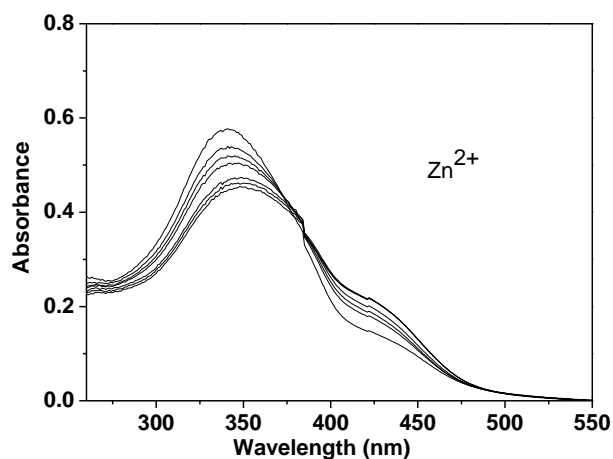


Figure S67. UV-vis absorption spectra of polymer **2** (13 μg/mL) with addition of various concentrations of Zn(OTf)₂ (0, 0.8595, 1.7049, 2.5366, 3.7590, 4.9524, 6.5 and 8 μM, respectively) in 2.4 mL DMSO: H₂O (4: 1 v/v) solution.

Polymer **2** in DMSO: H₂O (1: 1 v/v) solution:

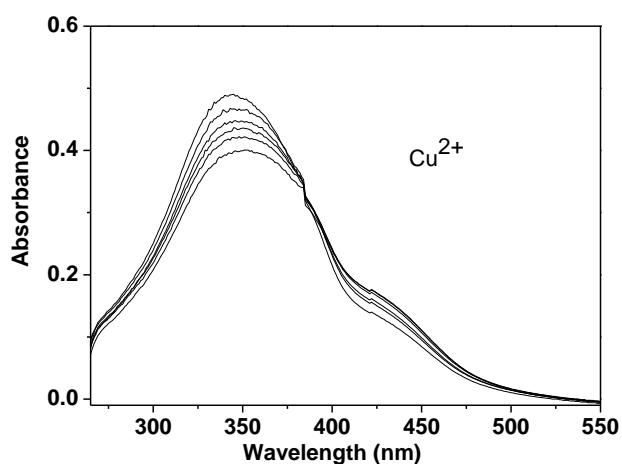


Figure S68. UV-vis absorption spectra of polymer **2** (13 μg/mL) with addition of various concentrations of Cu(OTf)₂ (0, 0.8595, 1.7049, 2.9473, 4.16 and 6.5 μM, respectively) in 2.4 mL DMSO: H₂O (1: 1 v/v) solution.

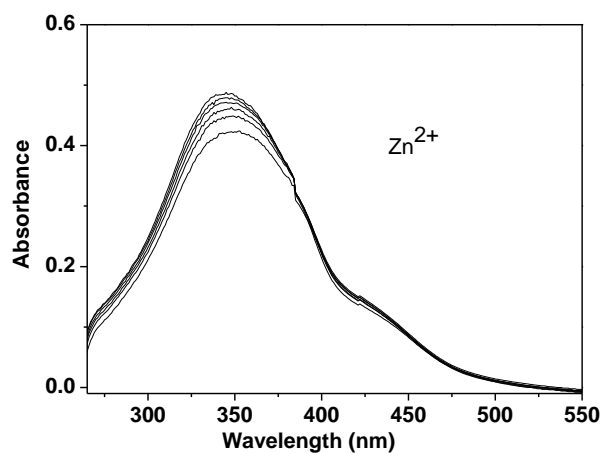


Figure S69. UV-vis absorption spectra of polymer **2** (13 $\mu\text{g}/\text{mL}$) with addition of various concentrations of $\text{Zn}(\text{OTf})_2$ (0, 0.8595, 1.7049, 2.9473, 4.16 and 6.5 μM , respectively) in 2.4 mL DMSO: H_2O (1: 1 v/v) solution.

Compound **3** in DMSO solution:

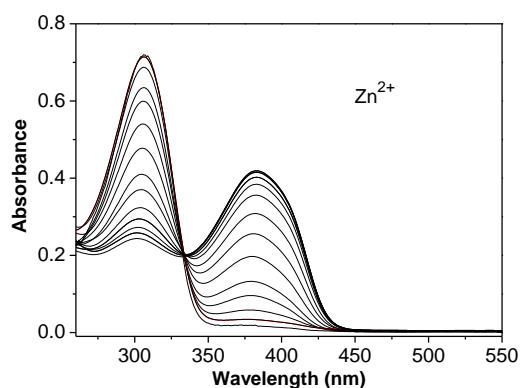


Figure S70. UV-vis absorption spectra of compound **3** (4.66 $\mu\text{g}/\text{mL}$) with addition of various concentrations of $\text{Zn}(\text{OTf})_2$ (0, 0.41, 1.23, 2.04, 2.83, 4.00, 5.14, 6.25, 7.33, 8.74, 10.45, 12.08 and 13.66 μM , respectively) in 2.4 mL DMSO solution.

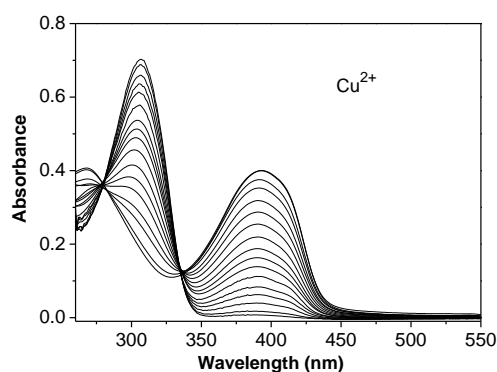


Figure S71. UV-vis absorption spectra of compound **3** (4.66 μg/mL) with addition of various concentrations of Cu(OTf)₂ (0, 0.41, 1.23, 2.04, 2.83, 4.00, 5.14, 6.25, 7.33, 8.74, 10.45, 12.08, 13.66, 15.49, 17.27, 18.91 and 20.26 μM, respectively) in 2.4 mL DMSO solution.

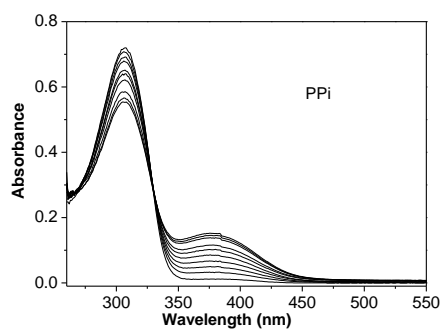


Figure S72. UV-vis absorption spectra of compound **3** (4.66 μg/mL) with addition of various concentrations of PPI (0, 41.32, 81.96, 2.04, 121.95, 180.72, 238.09, 294.11, 366.79, 437.26 and 505.61 μM, respectively) in 2.4 mL DMSO solution.

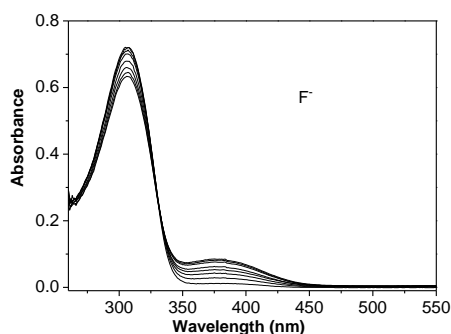


Figure S73. UV-vis absorption spectra of compound **3** (4.66 μg/mL) with addition of various concentrations of Bu₄NF (0, 41.32, 81.96, 2.04, 121.95, 180.72, 256.92, 330.74 and 402.30 μM, respectively) in 2.4 mL DMSO solution.

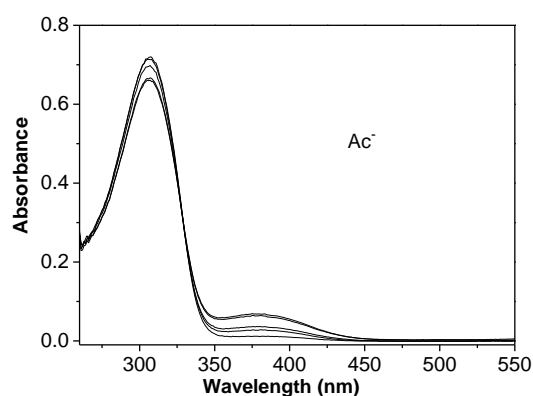


Figure S74. UV-vis absorption spectra of compound **3** (4.66 $\mu\text{g/mL}$) with addition of various concentrations of $\text{Bu}_4\text{N}^+\text{Ac}^-$ (0, 41.32, 81.96, 102.04 and 487.80 μM , respectively) in 2.4 mL DMSO solution.

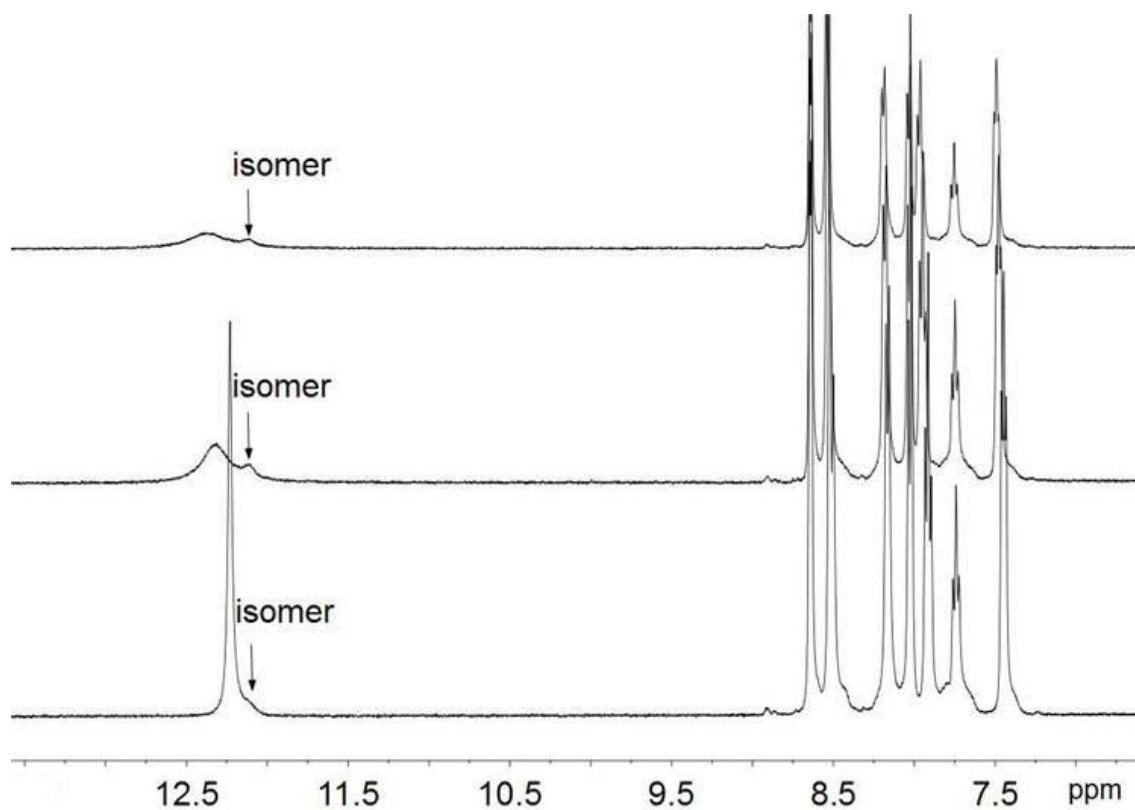


Figure S75. ^1H NMR spectra of compound **3** (bottom), **3** with 1 equiv. of $\text{Zn}(\text{OTf})_2$ (middle), and **3** with 2 equiv. of $\text{Zn}(\text{OTf})_2$ (top) in DMSO-d_6 . The minor *cis*-isomer is labelled.

Compound **3** in DMSO: H₂O (1: 1 v/v) solution:

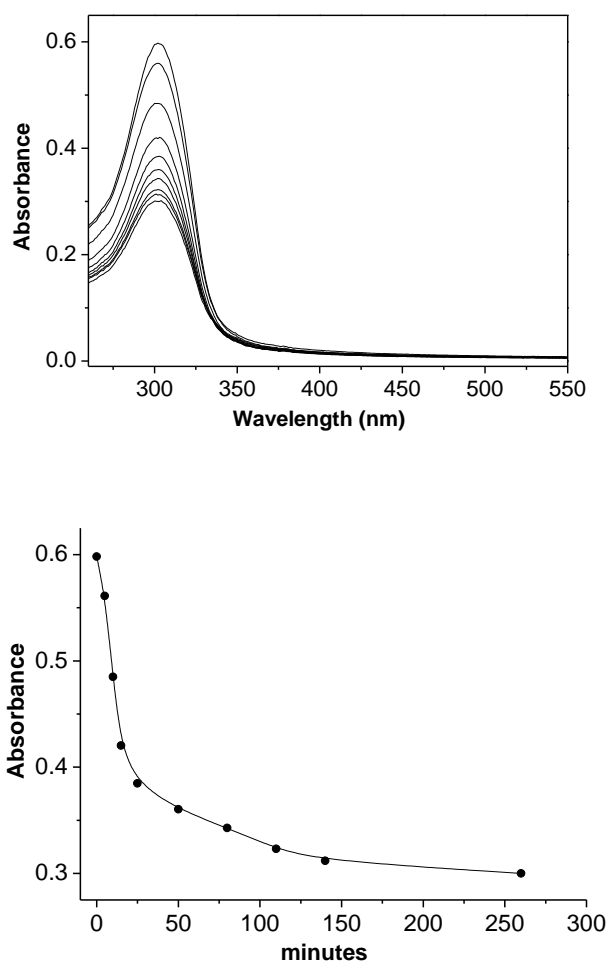


Figure S76. UV-vis absorption spectra of compound **3** (4.66 $\mu\text{g/mL}$) in 2.4 mL H₂O solution. As the time increased, the absorbance decreased.

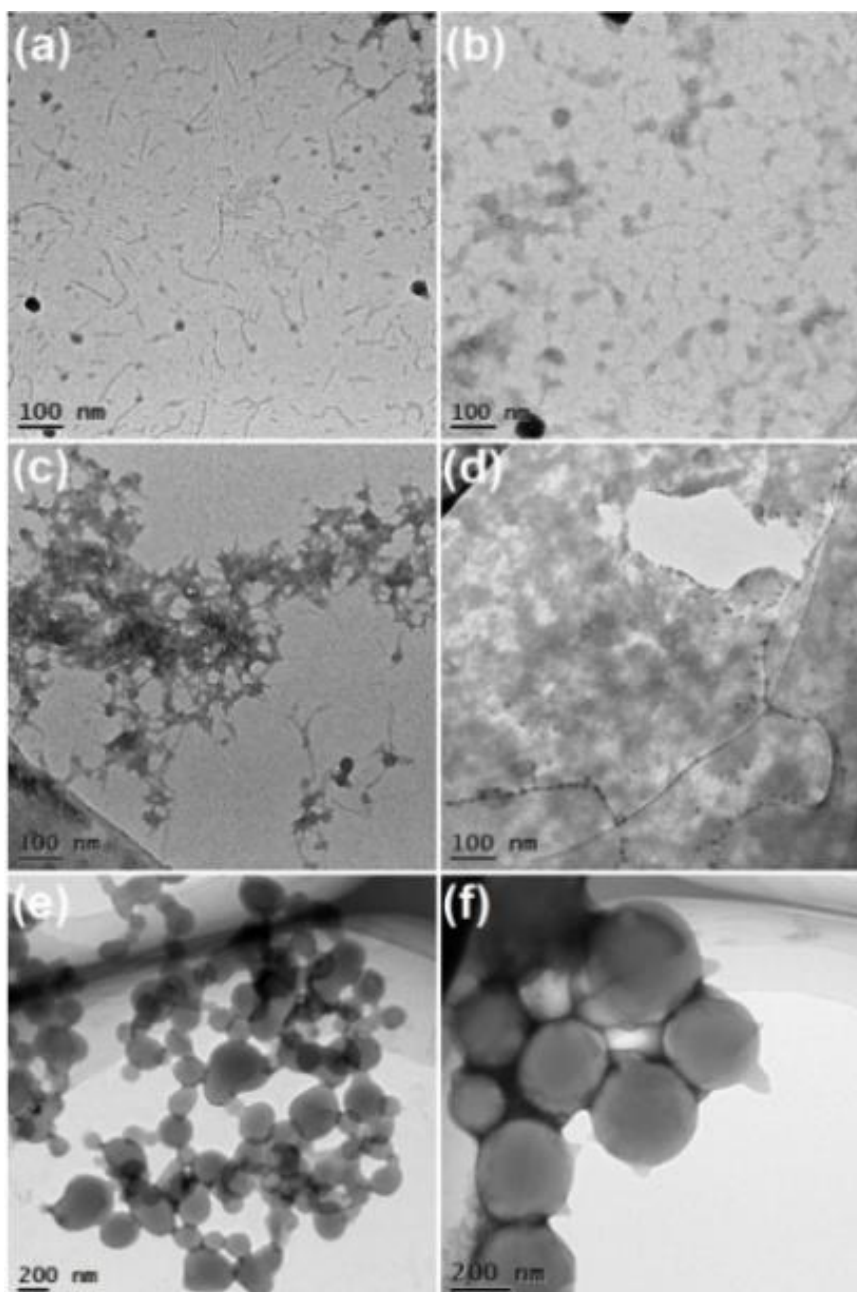


Figure S77. TEM images of **1** (44.8 $\mu\text{g/mL}$) in 4: 1 DMSO/ H_2O (a), **1** (44.8 $\mu\text{g/mL}$) in 1: 1 DMSO/ H_2O (b), **1** (44.8 $\mu\text{g/mL}$) in H_2O (c), **1** (44.8 $\mu\text{g/mL}$) and $\text{Cu}(\text{OTf})_2$ (150 μM) in H_2O (d), **2** (42 $\mu\text{g/mL}$) in 4: 1 DMSO/ H_2O (e), and **2** (42 $\mu\text{g/mL}$) and $\text{Cu}(\text{OTf})_2$ (150 μM) in 4: 1 DMSO/ H_2O (f).

Reference

- (1) Meng, W.; Ronson, T. K.; Clegg, J. K.; Nitschke, J. R. Transformations within a Network of Cadmium Architectures. *Angew. Chem. Int. Ed.* **2013**, *52*, 1017-1021.